AL-PHA beads: bioplastic-based protease biosensors for global health applications

Richard J. R. Kelwick[1,#], Alexander J. Webb[1,#], Yizhou Wang[1,#], Amelie Heliot[1], Fiona Allan[2], Aidan M. Emery[2], Michael R. Templeton[3] and Paul S. Freemont[1,4,5*]

[1]Section of Structural and Synthetic Biology, Department of Infectious Disease, Imperial College London, London, SW7 2AZ, UK. [2]Department of Life Sciences, Natural History Museum, London, SW7 5BD, UK. [3]Department of Civil and Environmental Engineering, Imperial College London, SW7 2AZ, UK. [4]The London Biofoundry, Imperial College Translation & Innovation Hub, White City Campus, 80 Wood Lane, London W12 0BZ, UK. [5]UK Dementia Research Institute Care Research and Technology Centre, Imperial College London, Hammersmith Campus, Du Cane Road, London, W12 0NN

[#]Joint First Authors. *To whom correspondence should be addressed:

Prof Paul Freemont:
Section of Structural and Synthetic Biology, Department of Infectious Disease, Sir Alexander Fleming Building, South Kensington Campus, Exhibition Road, London, SW7 2AZ, UK
Email: p.freemont@imperial.ac.uk, Tel: +44 (0) 207 594 5327

ABSTRACT

Proteases are multi-functional, proteolytic enzymes that have complex roles in human health and disease. Detecting the activities of proteases can lead to important insights into communicable and non-communicable diseases. Therefore, the development of protease detection strategies can be beneficial to an array of global health applications. To this end, we developed **A**dvanced proteo**L**ytic detector **P**oly**H**ydroxy**A**lkanoates (AL-PHA) beads – a library of low-cost, biodegradable, bioplastic-based protease biosensors. Broadly, these biosensors utilise PhaC-reporter fusion proteins that are bound to microbially manufactured polyhydroxyalkanoate (PHA) bioplastic beads. These PhaC-fusions also incorporate modular specific protease cleavage sites. In the presence of a specific protease, superfolder green fluorescent (sfGFP) reporter proteins are cleaved off of the AL-PHA beads - resulting in a loss of bead fluorescence. These AL-PHA biosensors were initially optimised using a commercially available Tobacco Etch Virus (TEV) protease. Our third generation TEV biosensor (PhaC-112L-T-G) detected 0.5 U (1.85 pM) of AcTEV activity and 10 units of AcTEV protease activity resulted in a visually noticeable loss in AL-PHA bead fluorescence. AL-PHA beads also detected cercarial elastase from *Schistosoma mansoni*-derived cercarial transformation fluid (SmCTF) samples, as well as cancer-associated metalloproteinases in extracellular vesicle and cell-conditioned media samples. We envision that AL-PHA beads could be adapted towards a low-cost and high-throughput protease detection assay for global health applications.

Keywords: protease biosensor, polyhydroxyalkanoates, *Schistosoma mansoni*, cercarial elastase, metalloproteinase, extracellular vesicles, global health

Running Title: Bioplastic-based protease biosensors

Introduction

Synthetic biology is an established scientific field, based upon engineering design principles, that has led to innovations in the development of biosensors and bioreporters geared towards global health applications [1–3]. Synthetic biology biosensors and bioreporters have been successfully developed to help detect drinking water contaminants [4], environmental or industrial pollutants [5] and disease biomarkers [6,7]. These diverse applications have inspired a multitude of biosensor designs that have innovated beyond typical electrochemical formats, towards whole-cell bioreporters (WCBs) and cell-free biosensors [8–11]. More recently, convergences between the materials sciences and synthetic biology are opening up new opportunities for global health biosensor applications [12]. In particular, we envisage that functionalised biomaterials may enable the emergence of novel strategies for detecting biomedically important proteases [13].

Proteases are multi-functional proteolytic enzymes, that have complex roles in human health and disease [14]. Protease functions are diverse and can be broad, such as aiding food digestion, or highly evolved and specialised targeting more specific substrates [15,16]. Exemplars of proteases that have evolved to serve complex biological functions can be found within the matrix metalloproteinase (MMP), the A Disintegrin And Metalloproteinase (ADAM) and A Disintegrin and Metalloproteinase with Thrombospondin motifs (ADAMTS) protease families [17]. Members of these protease families contribute to an array of biological processes including: cellular metabolism, cell-signalling, cell-migration, immunomodulation and tissue remodelling [18–22]. Changes in human metalloproteinase gene expression and/or their proteolytic activities can lead to cardiovascular or inflammatory pathologies, neurodegenerative diseases, changes in immunoregulation and cancer [23–27]. Proteases also have important roles in communicable diseases, whereby infectious microorganisms and

parasites employ proteases to support pathogenesis [28]. In the case of schistosomiasis (also known as bilharzia or snail fever), a neglected tropical disease that affects over 250 million people worldwide [29–31], the invasive *Schistosoma* cercariae release a cocktail of proteases, including elastase, that help the parasite to invade into a host through the skin [32,33].

Evidently, understanding the activities of proteases can lead to important insights into communicable and non-communicable diseases [34,35]. Indeed, novel protease detection strategies, especially those intended for field use, may be beneficial to many different clinical, biotechnological, environmental and epidemiological global health applications [13,36–39]. For example, in our previous study we used a synthetic biology approach to engineer *Escherichia coli* and *Bacillus subtilis* WCBs that can detect the elastase activity from the cercariae of the parasite *Schistosoma mansoni* [11]. Importantly, our study demonstrated the detection of the proteolytic activity of a specific protease (i.e. cercarial elastase) within complex biological samples. However, the implementation of WCBs within global health settings is challenging and many other complex practical, cultural, societal, data protection and regulatory concerns must also be addressed [3,40]. Understandably, amongst those concerns, the accidental release of living engineered WCBs is commonly cited [41]. In response to these challenges, the development of WCBs has led to important innovations in physical (e.g. sealing WCBs within devices) and genetic (e.g. genetically encoded kill switches or auxotrophy) containment strategies, that help mitigate the risk of accidental release [42–44]. Whilst these bacterial containment strategies are impressive, we anticipate that non-living biosensors may be desirable in certain contexts. To this end, we developed modular, functionalised, polyhydroxyalkanoates (PHAs)-based, bioplastic beads for protease detection. We termed these biosensor beads - **A**dvanced proteo**L**ytic detector **PHA**s (**AL-PHA**) beads, and initially optimised their design using a commercially available Tobacco Etch Virus (TEV) protease. As

proof-of-concept that AL-PHA beads can be applied to global health applications, AL-PHA biosensors were assayed against *S. mansoni* derived samples containing soluble cercarial antigens, termed cercarial transformation fluid (SmCTF). AL-PHA biosensors successfully detected cercarial elastase activity within these samples. As additional global health exemplars, AL-PHA beads were also engineered to detect cancer-associated metalloproteinases including: MMPs, ADAMs and ADAMTSs. Most notably, AL-PHA beads detected recombinant MMP14 and extracellular vesicle (EV)-associated ADAM10 derived from an *in vitro* model of non-small cell lung cancer (nsclc). Furthermore, we also demonstrate the potential use of AL-PHA beads in a high-throughput screening context - whereby an entire library of metalloproteinase biosensors were tested in parallel. To the best of our knowledge, this proof of concept study is the first to demonstrate the use of functionalised PHAs-based protease biosensors for global health applications.

Results and discussion

The polyhydroxyalkanoates (PHAs) are biopolymers that are naturally synthesised in many different bacterial, fungal and archaeal species [45,46]. PHAs producing microorganisms typically utilise PHAs as an energy source, a carbon store, or for protection against hydroxyl radicals [47]. Differences in PHAs biosynthetic operons, metabolic pathways and ecological niches across different PHAs producing microorganisms influence which PHAs biopolymers are produced [48–50]. PHAs polymers have also been bio-manufactured within microbial cell factories [51]. These natural or engineered PHAs represent a diverse family of biopolymers with different mechanical characteristics, thermal properties, biodegradabilities and biocompatibilities [48,52,53]. Poly-3-hydroxybutyrate (P(3HB)) is one of the most well studied PHAs polymers and can potentially be used within food packaging or for other

industrial applications [54,55]. P(3HB) is also biocompatible, which enables its use in medical and tissue engineering applications [56]. These industrial and biomedical applications have inspired decades of innovative metabolic engineering, biotechnology and synthetic biology strategies for enhancing PHAs production [12,57]. Most notably, refactoring of the native *phaCAB* operon from *Cupriavidus necator* has led to significant improvements in P(3HB) production in engineered *E. coli* [58–60]. In our previous studies, we developed synthetic biology, model-guided design and cell-free prototyping strategies to engineer and optimise the microbial production of PHAs bioplastics [59,61]. Once generated, these *phaCAB* engineered *E. coli* were typically cultured in media containing excess carbon (e.g. glucose or whey permeate) in order to boost intracellular levels of acetyl-CoA [59,61,62]. Acetyl-CoA can then feed directly into P(3HB)-producing *phaCAB* biosynthetic operons (Fig. 1A). Initially, acetyl-CoA is processed by PhaA (3-ketothiolase) to form acetoacetyl-CoA. Subsequently, PhaB (acetoacetyl-CoA reductase) reduces acetoacetyl-CoA to form the monomer (*R*)-3-hydroxybutyl-CoA ((*R*)-3HB-CoA). Finally, (*R*)-3HB-CoA is polymerised by PhaC (PHA synthase) to form the final PHAs polymer - P(3HB). This P(3HB) polymer naturally forms into spherical granules (beads) within engineered *E. coli* [63].

Interestingly, these PHAs beads can also be functionalised *in vivo* with engineered fusion proteins, which decorate the materials surfaces [64]. Such functionalised PHAs beads have enabled novel protein purification strategies [65], as well as the development of PHAs-based vaccines [66]. Indeed, insights from previous studies have demonstrated that post purification, PhaC remains bound to the bead surface [67]. We, therefore reasoned that we could display highly engineered PhaC-fusion proteins, which could act as protease biosensors, on the surfaces of these PHAs beads (AL-PHA beads). To this end, a highly active C104 *phaCAB* biosynthetic operon was selected, from our previous studies, as the foundation from which to

develop AL-PHA producing operons in engineered *E. coli* [59,61]. These AL-PHA operons contain PhaC-fusion proteins which have been designed to incorporate a flexible amino acid linker, interchangeable (modular) protease-specific cleavage sites, and a reporter protein (Fig. 1A & 1B; Fig. 2A; Supplementary Tables 1-4; Supplementary Fig. 1). By changing the protease-specific sites in the PhaC-fusion proteins, to those recognised by specific proteases (e.g. cercarial elastase or metalloproteinases), a suite of AL-PHA bead biosensors can be generated (Supplementary Fig. 2; Supplementary Table 1). These fusion proteins were designed such that specific proteases can be detected via the recognition of the cleavage site and subsequent proteolytic removal of the reporter protein (superfolder green fluorescent protein – sfGFP), from the surface of the AL-PHA beads.

AL-PHA beads were produced in appropriately engineered *E. coli* cells and isolated using a sonication-based method (See materials and methods). We also developed a straightforward AL-PHA biosensor assay (Fig. 1C). Essentially, control or protease specific AL-PHA beads were incubated with protease samples. Incubation temperatures, reaction durations and assay buffers are largely dependent upon the optimal activity requirements of the proteases being detected (See materials and methods). Post-incubation, AL-PHA assay samples were centrifuged to pellet AL-PHA beads and to ensure separate sampling of the assay supernatant from the AL-PHA beads themselves. Importantly, this means that for highly active proteases, AL-PHA assays can be assessed both in terms of whether sfGFP has been proteolytically released into the assay supernatant (plate reader assay) and whether there is a concomitant loss in AL-PHA bead fluorescence (flow cytometry assay).

Localisation of PhaC-sfGFP fusion proteins on the AL-PHA bead surface was initially validated using a trypsin treatment assay. We reasoned that if the fusion proteins are correctly

designed, such that they are exposed and accessible to the external environment, then trypsin will non-specifically cleave and degrade the fusion proteins, resulting in decreased AL-PHA bead fluorescence. As expected, trypsin treatment (1 μg) significantly decreased AL-PHA bead fluorescence compared to untreated controls (0 μg; Supplementary Fig. 3). Usefully, this reduction in bead fluorescence was observable to the naked eye when the beads were pelleted then placed onto a transilluminator (Supplementary Fig. 3C). Thus, these data demonstrate that our engineered PhaC-fusion proteins are correctly localised on the surfaces of AL-PHA beads and are susceptible to proteolytic activity. The trypsin assay also enabled us to establish the flow cytometry protocols and gating strategy used in all subsequent AL-PHA biosensor assays (See materials and methods; Supplementary Fig. 4).

In order to optimise the performance of AL-PHA biosensors, three different biosensor generations (designs) were developed that differ in terms of the length of the flexible amino acid linker region (Fig. 2A; Supplementary Table 2). We previously identified that longer linker lengths can increase biosensor sensitivity, likely through improving protease cleavage site access [11]. We therefore, chose three flexible linker lengths namely twelve amino acids (12L; first generation); twenty-two amino acids (22L; second generation); one hundred and twelve amino acids (112L; third generation). A representative plasmid map showing the sequence of the third generation TEV specific AL-PHA biosensor (PhaC-112L-T-G) is shown in Supplementary Fig. 1.

First (Fig. 2B), second (Fig. 2C) and third generation (Fig. 2D) controls and TEV AL-PHA biosensors were assayed with either 0 or 10 U of AcTEV protease and incubated at 30^{o}C for 2 hours with shaking. Post-assay supernatants and AL-PHA beads were assessed, separately, using either plate reader (supernatant) or flow cytometry (AL-PHA bead) workflows. In comparison to untreated controls (0 U AcTEV), supernatant fluorescence levels increased for

all AcTEV treated (10 U) TEV specific AL-PHA bead samples - indicating that all three biosensor generations can detect AcTEV protease and function as biosensors (Figures 2B-D). However, the third generation TEV specific AL-PHA biosensor (PhaC-112L-T-G) was the most sensitive. Indeed, relative supernatant fluorescence levels increased 10.21 ±1.2-fold on average (Fig. 2D), which we quantified using a GFP calibration curve as being equivalent to 1.87 μM sfGFP being released (Supplementary Fig. 5). These GFP calibration and flow cytometry data (Fig. 2D; Supplementary Fig. 5) also enable us to estimate that this equates to ~37 pmoles of GFP being released from ~302,000 AL-PHA beads, which is within the range of previous granule surface protein coverage estimates [65,68]. Whilst, as expected, the supernatant fluorescence levels of control biosensor samples were unchanged by AcTEV (10 U) treatment (Figures 2B-D).

Furthermore, the concomitant reduction in AL-PHA bead fluorescence was also significantly more pronounced for the third generation AL-PHA TEV specific biosensor design (-0.49 ±0.12 [~49% decrease]; Fig. 2D) and this reduction in bead fluorescence was also observable, using a transilluminator, to the naked eye (Supplementary Fig. 6). Increasing the duration of AcTEV treatment to 6 h reduced third generation AL-PHA bead fluorescence even further (-0.71 ±0.18 [~71 % decrease]; Fig. 3A), but did not result in the complete removal of all AL-PHA fusion proteins. Therefore, we reasoned that shorter AL-PHA assays (2-4 h) were sufficient and more practical. Indeed, after 2 hours of treatment AL-PHA beads (PhaC-112L-T-G) are sensitive enough to detect 0.5 U of AcTEV activity (Fig. 3B), which we estimate to be around 1.85 pM of AcTEV protease.

Taken together, these data demonstrate that third generation AL-PHA beads were the most sensitive biosensor design. These data are in accordance with our previously used biosensor design optimisation strategy, in which increasing the flexible amino acid linker improved protease cleavage site access [11]. Furthermore, in concordance with previous PHAs

functionalisation studies (e.g. PHAs-based protein purification [63]) our third generation AL-PHA beads were robust for at least 12-months post-production. More specifically, AL-PHA beads remained visibly fluorescent (Supplementary Fig. 7) and we anticipate that AL-PHA bead robustness will be useful for downstream field and point-of-care applications.

We next cloned a panel of third generation AL-PHA protease biosensors designed to detect cercarial elastase or metalloproteinases, including select MMPs, ADAMs and ADAMTSs (See materials and methods; Supplementary Table 3). Several batches of these different AL-PHA beads were generated in engineered *E. coli* and purified using a sonication-based method (See materials and methods). AL-PHA bead sizes were characterised using dynamic light scattering (DLS) and were typically 1.1 ±0.02 μm in diameter (Supplementary Fig. 8A). Flow cytometry was also used to confirm that that these third generation AL-PHA bead biosensors had been correctly assembled *in vivo*. Essentially, all third generation AL-PHA beads were typically ~30-48 fold more fluorescent than the non-functionalised control PHAs beads (C104), which indicates correct fusion protein assembly and surface localisation (Supplementary Fig. 8B). In contrast, the MMP9 (PhaC-112L-P9-G) and elastase (PhaC-112L-E-G) specific AL-PHA beads were only ~4 fold more fluorescent than control beads (C104). These differences in AL-PHA bead fluorescence suggest that certain protease recognition motifs (cleavage sites) within the fusion proteins may influence sfGFP folding. However, the modular nature of the AL-PHA biosensors means that future design iterations could enhance these biosensors and improve their protein folding/structural folding. Nevertheless, our flow cytometry data indicate that all third generation AL-PHA beads were functionalised and suitable for application testing.

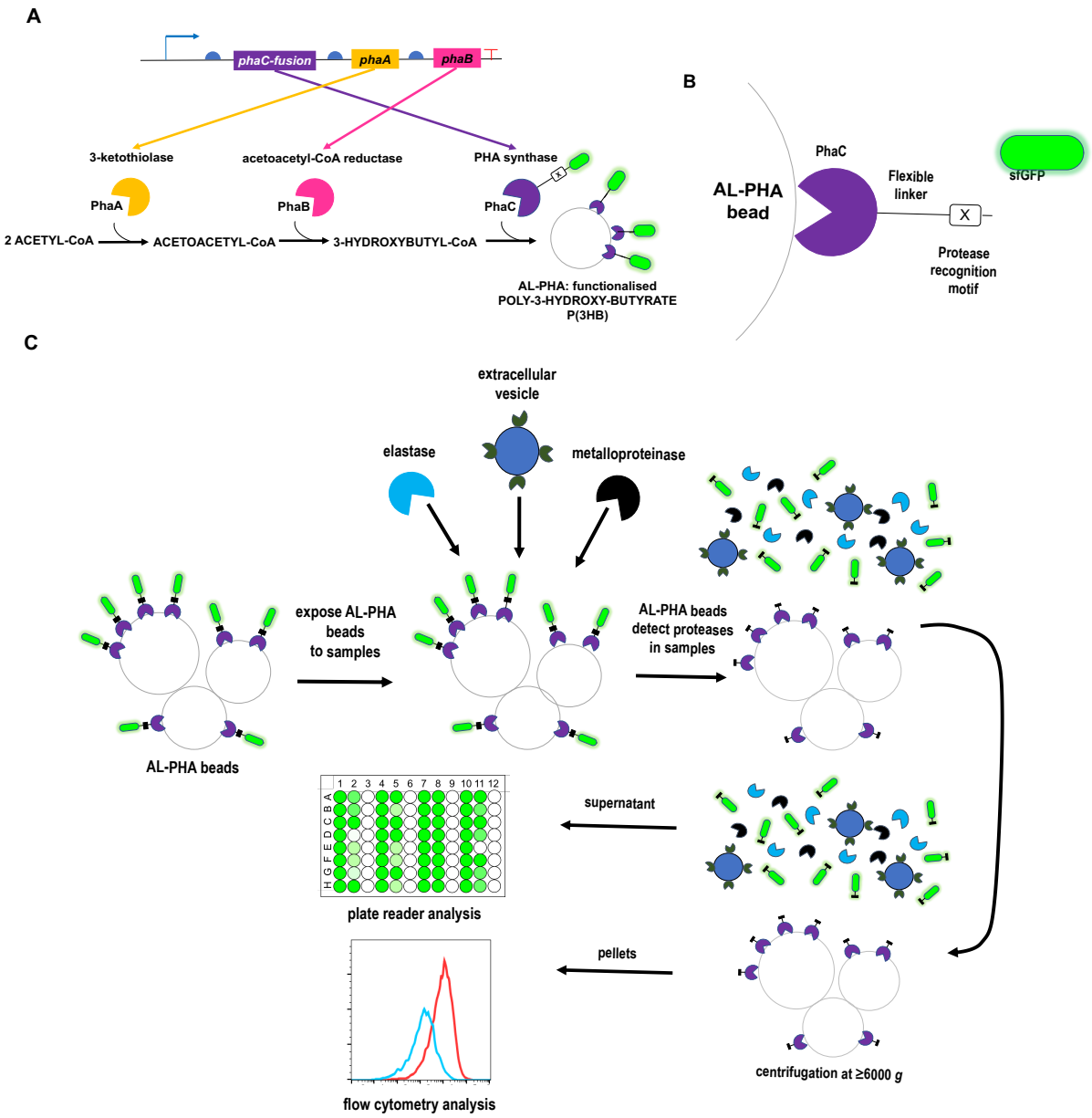

Figure 1 Advanced proteoLytic detector PolyHydroxyAlkanoates (AL-PHA) beads and protease biosensor assay workflow. (A) Schematic of the *phaCAB* biosynthetic operon and the enzymatic pathway used for production of AL-PHA biosensor beads in engineered *Escherichia coli*. **(B)** AL-PHA bead and fusion protein design **(C)** AL-PHA biosensor assay workflow.

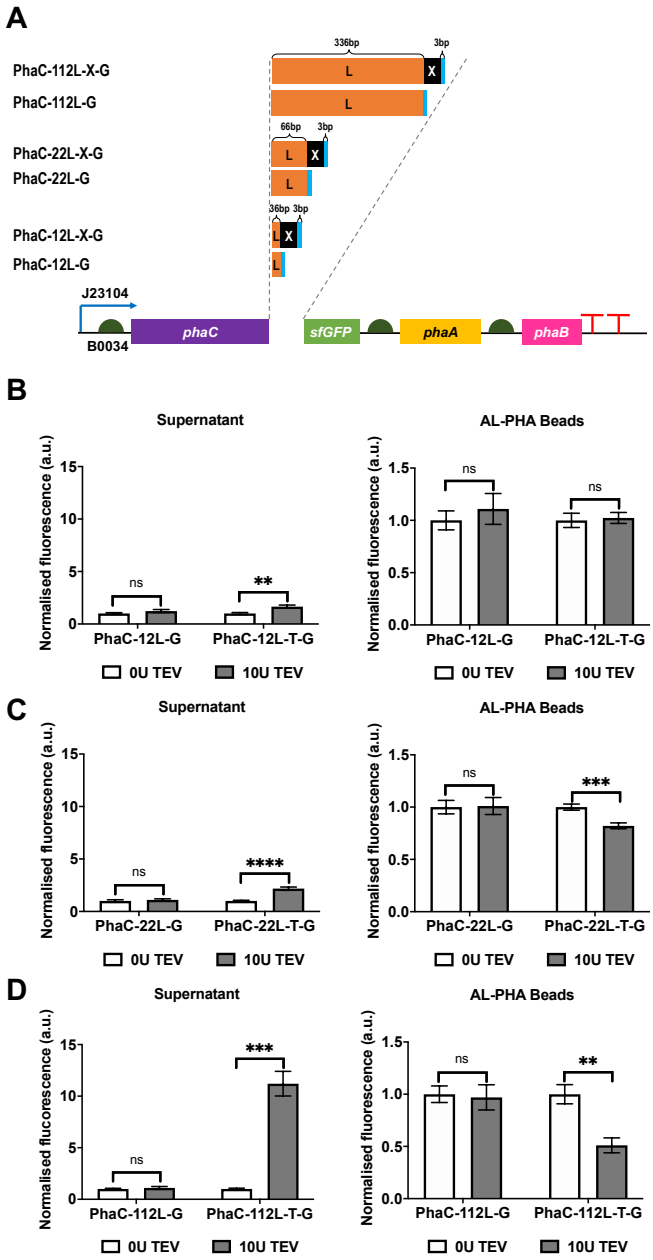

Figure 2 AL-PHA biosensor design optimisation. (A) Schematic of engineered *phaCAB* operons for production of first, second and third generation control and protease detection AL-PHA biosensors. Abbreviations: 12L, 22L and 112L denote the amino acid length of the flexible linker, X denotes the protease recognition motif site for either TEV (T), cercarial elastase (E) MMP (P), ADAM (M) or ADAMTS (TS) proteases and G denotes superfolder green fluorescent protein (sfGFP). Analysis of first **(B)**, second **(C)** and third generation **(D)** control and TEV protease AL-PHA biosensors. AL-PHA biosensors were treated with either 0 units (0 U) or 10 units (10 U) of AcTEV protease. Proteolytically released sfGFP in supernatant samples were analysed using a CLARIOstar plate reader (483-14 nm/530-30nm) and these fluorescence data were normalised against untreated controls of the same biosensor batch. AL-PHA beads were analysed using flow cytometry (Attune, Life Technologies, USA) and AL-PHA bead geometric mean (BL1-A, 488nm/530-30nm) of AcTEV treated beads were normalised against untreated controls of the same biosensor batch. Error bars denote standard error of the mean, n=4-8, Student *t*-test **P<0.01, ***P<0.001, ****P<0.0001or not statistically significant (ns).

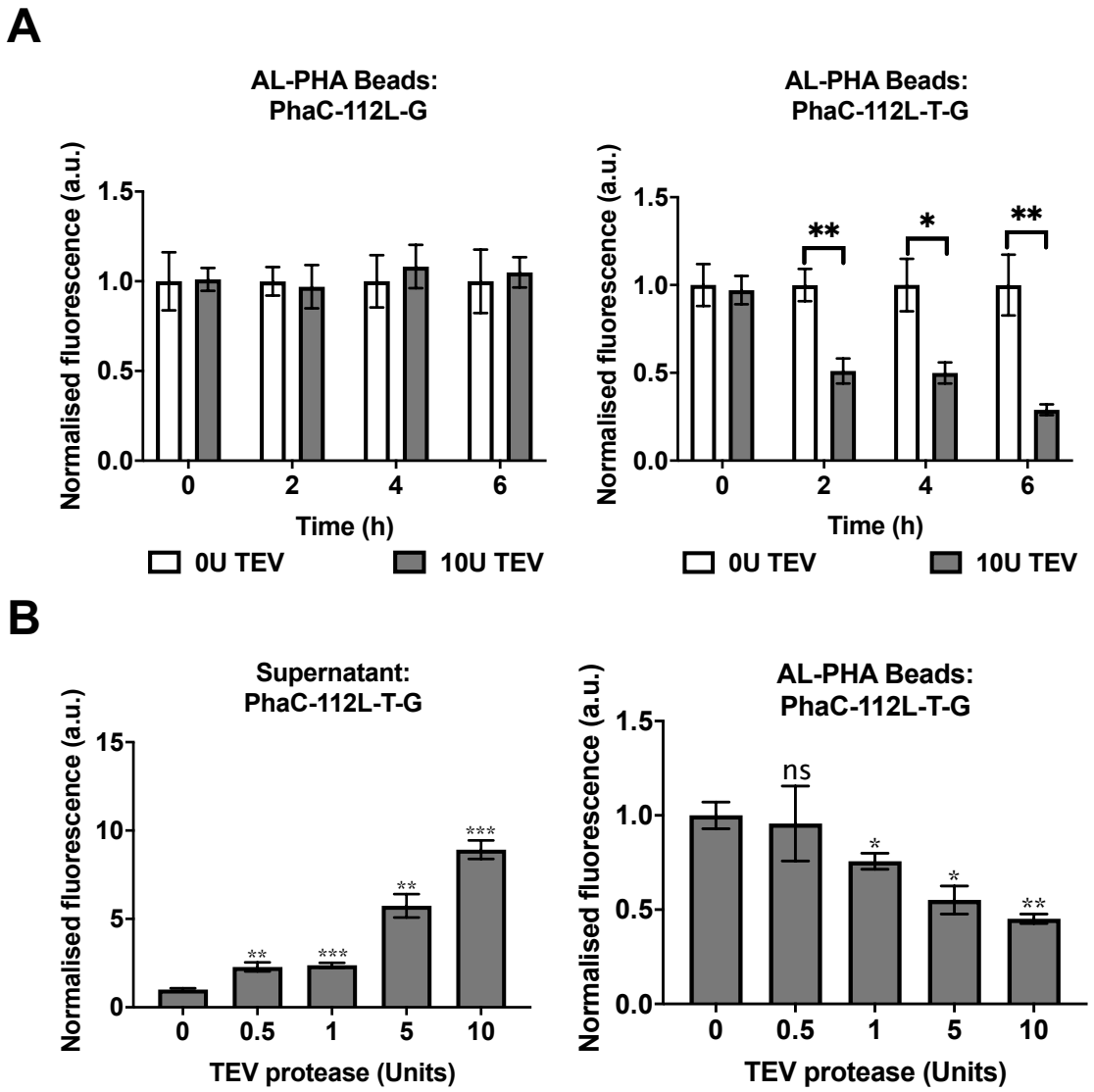

Figure 3 AL-PHA biosensor assay development. (A) Time course assay. Control (PhaC-112L-G) and TEV (PhaC-112L-T-G) AL-PHA biosensor beads were incubated with 0 (0 U) or 10 units (10 U) of AcTEV protease for 0-6 hours. AL-PHA beads were analysed using flow cytometry and AL-PHA bead geometric mean (BL1-A, 488nm/530-30nm) of TEV treated beads were normalised against untreated controls of the same biosensor batch. **(B)** AL-PHA biosensor sensitivity. AL-PHA TEV biosensors were incubated for 2 hours with 0-10 units of AcTEV protease. Supernatant fluorescence data (483-14 nm/530-30nm) were normalised against untreated controls of the same biosensor batch. AL-PHA beads were analysed using flow cytometry and the geometric mean of TEV treated AL-PHA biosensor beads were normalised against untreated controls of the same biosensor batch. Error bars denote standard error of the mean, n=3-4 (AL-PHA batches), Student *t*-test *P<0.05, **P<0.01, ***P<0.001 or not statistically significant (ns).

Schistosoma mansoni cercarial elastase detection

The neglected tropical disease schistosomiasis is of increasing burden to global health, with estimates suggesting that 779 million people are at risk of infection leading to an annual mortality upwards of 280,000 people in sub-Saharan Africa alone [29,30,69]. To show that the AL-PHA assay is applicable to a global health issue, we engineered AL-PHA beads that could detect *S. mansoni* – one of the principal causative agents of schistosomaisis. Previously, we have specifically targeted the *S. mansoni* cercarial elastase activity as our marker for detection using WCB's [11]. The cercariae utilise this elastase activity to penetrate the skin barrier, thereby enabling invasion and infection of their definitive hosts, in this case humans [32,33].

Using plasmid pYZW40 as a template and primer pair AJW671/AJW672 (Supplementary Table 3, Supplementary Table 4), the TEV protease recognition motif was replaced with that of *S. mansoni* cercarial elastase via inverted PCR. As we discuss later, this generalised PCR strategy was also used to create a panel of metalloproteinase AL-PHA biosensors (Supplementary Table 3, Supplementary Table 4). The *S. mansoni* cercarial elastase specific recognition motif (-SWPL-) used here and in our previous study [11], was identified using positional scanning – synthetic combinatorial library screening [33]. To test whether our AL-PHA design could detect elastase, we tested three biologically distinct *S. mansoni*-derived samples containing soluble cercarial antigens, termed cercarial transformation fluid (SmCTF; Fig. 4A) [70]. These samples were obtained by mechanically transforming cercariae released from the intermediate snail host, *Biomphalaria glabrata* (Fig. 4A) [70]. When the elastase specific AL-PHA beads were exposed to the SmCTF samples, the beads detected elastase in SmCTF samples 2 and 3, as evidenced by the increase in supernatant sfGFP fluorescence and a reduction in sfGFP bead fluorescence (Fig. 4B). Although SmCTF1 caused a slight reduction in bead fluorescence, no corresponding increase in supernatant fluorescence was detectable

(Fig. 4B), suggesting that this sample has lower amounts of elastase. We did however, observe some off-target cleavage for the three SmCTF samples against the TEV protease control beads (Fig. 4B). This may be due to the way the SmCTF samples were obtained [70,71]. Indeed, these gland extracts contain both elastase and various other proteases [72–74]. We do not know if these peptidases or other gland contents are responsible for the off-target effects, however, it is evident that for at least two of the SmCTF samples, the elastase specific AL-PHA beads are cleaved significantly more (Fig. 4B).

The implementation of AL-PHA biosensors within resource-limited settings could be challenging and different practicalities, including those we have previously identified, must be considered [3,11]. Essentially, AL-PHA biosensors will need to be implemented within broader public health strategies (e.g. water, sanitation, and hygiene [WASH] [75]), which integrate appropriate stakeholder engagement, collaboration and sustainable programmes that improve access to safe water sources [4]. There are also practicalities around sample preparation that must be addressed. The level of cercariae that are present in infected water courses can vary greatly and therefore, any cercariae present in a collected water sample will need to be concentrated. Beneficially, several trap systems have been successfully devised that attract, capture and concentrate schistosoma cercariae ready for downstream sample processing [3,76,77]. Indeed, after concentration, low-cost, portable molecular biology equipment (e.g. Bento Lab [78,79]) and cell phone-based, hand-held plate readers [80] could feasibly facilitate AL-PHA biosensor assays in the field.

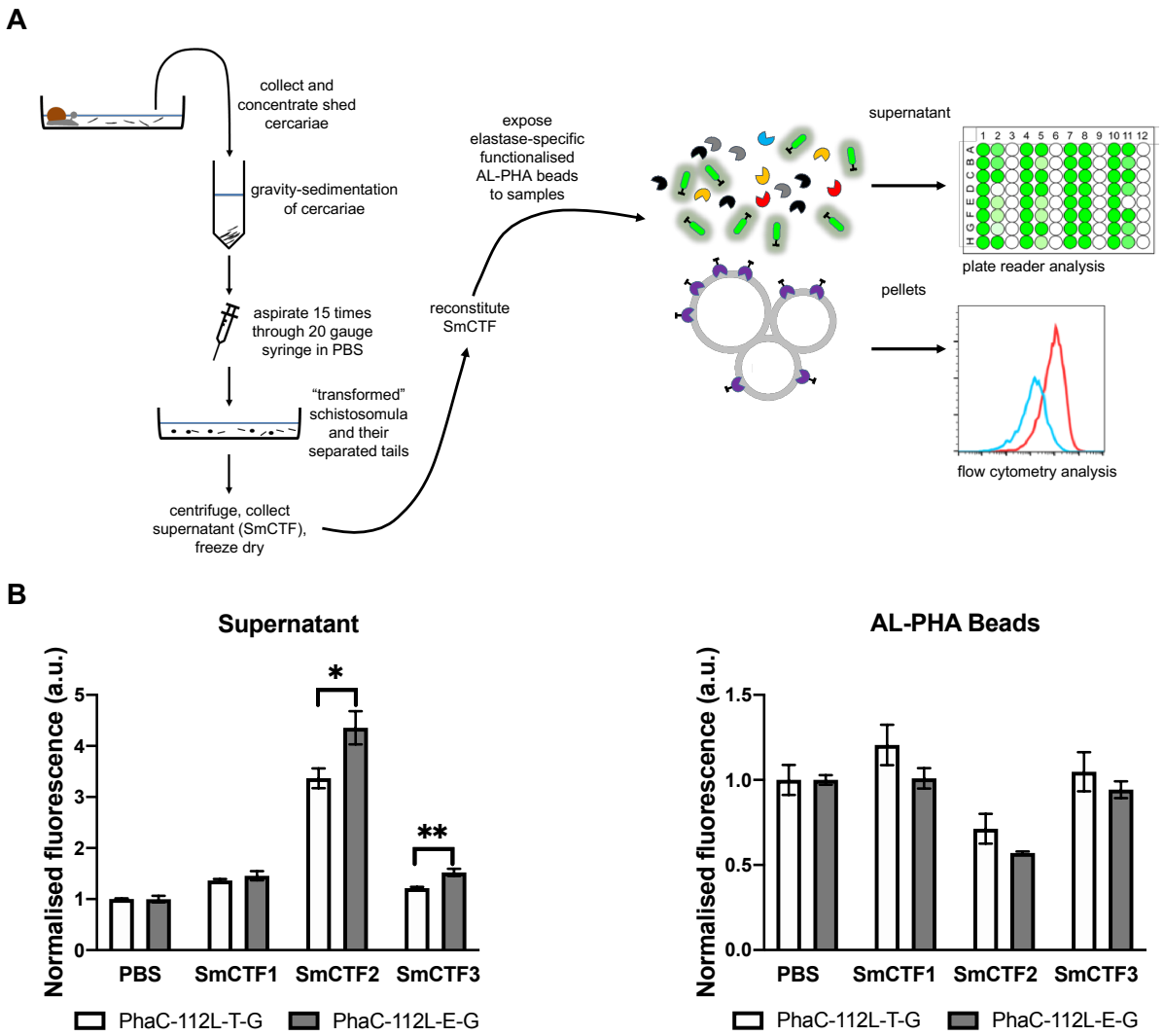

Figure 4 Detection of cercarial elastase in *Schistosoma mansoni* cercarial samples. (A) Cercarial elastase AL-PHA biosensor assay. *Schistosoma mansoni* cercariae were shed from infected snails, mechanically processed to produce *S. mansoni* cercarial transformation fluid (SmCTF) samples and then lyophilised in PBS (1X). Lyophilised SmCTF samples were reconstituted in water for AL-PHA biosensor assays. **(B)** AL-PHA TEV (PhaC-112L-T-G) and elastase (PhaC-112L-E-G) biosensors were treated with either PBS or SmCTF samples. Supernatant fluorescence data (483-14 nm/530-30nm) of SmCTF treated AL-PHA biosensors were normalised against mock-treated controls (PBS) of the same biosensor batch. AL-PHA beads were analysed using flow cytometry and the geometric mean (BL1-A, 488nm/530-30nm) of SmCTF treated AL-PHA biosensor beads were normalised against PBS controls of the same biosensor batch. Error bars denote standard error of the mean, n=3 (AL-PHA batches), Student *t*-test *P<0.05 and **P<0.01.

Metalloproteinase detection

The matrix metalloproteinases (MMPs) are a family of proteases that have important physiological roles in extracellular matrix (ECM) turn-over, tissue homeostasis, immunomodulation, and cell signalling [81]. There are 23 human MMPs and these proteases are often classified by their substrate specificities or domain architectures [81]. Additionally, a subset of MMPs, the membrane type MMPs (MT-MMPs) have a C-terminal glycophosphatidylinositol anchor (MT4- and MT6-MMP) or transmembrane domain (MT1-, 2-, 3- and MT5-MMP) that tethers them to the cell membrane [81,82]. Several MMPs and MT-MMPs have been implicated in cancer disease progression [83]. Interestingly, differential MT1-MMP (also called MMP14) expression or proteolytic activities can promote breast tumour cell migration, metastasis and tumour vascularisation [84]. Hence, within the context of breast cancer, the detection of MMP14 proteolytic activity might be highly informative. Therefore, the development of a low-cost AL-PHA biosensor that can detect MMP14 activity could be a useful biomarker research tool.

We therefore tested a MMP14-specific AL-PHA biosensor using recombinant MMP14 (Fig. 5). Prior to the start of AL-PHA biosensor assays, TPCK-trypsin (added to activate MMP14) was inactivated with aprotinin and additional aprotinin was also incorporated within MMP14 AL-PHA assay buffers. Control and MMP14-specific AL-PHA beads were treated with 0 μg or 0.55 μg (equivalent to 0 or 0.033 mU) of activated, recombinant MMP14 and assayed at 37^{o}C for 4 h (Fig. 5A). Relative sample supernatant fluorescence levels increased by 2.45 ±0.24-fold for MMP14 treated (0.55 μg) AL-PHA bead samples, when compared against untreated controls (0 μg) (Fig. 5B). These data indicate positive detection of MMP14 proteolytic activity. In contrast, relative supernatant fluorescence levels increased by just 0.77 ±0.21-fold in MMP14 treated (0.55 μg) control biosensor assays (PhaC-112L-G) (Fig. 5B).

Preliminary bioinformatics analysis, using CleavPredict software [85] highlighted a candidate MMP14 cleavage site (TGVVP-|-ILVEL) within the sfGFP reporter protein itself (close to N-terminal, amino acids 9-18) which might account for the observed off-target affects. For this current study, supernatant fluorescent data in tandem with concomitant AL-PHA bead analyses negated the off-target effects. Indeed, MMP14 treatment (0.55 μg) caused a significant decrease in MMP14 AL-PHA bead fluorescence (-0.26 ±0.08 [~26% decrease]; PhaC-112L-P14-G), whilst control AL-PHA beads (PhaC-112L-G) were unaffected (Fig. 5B). Taken together, the supernatant and AL-PHA bead data showed that our MMP14 AL-PHA biosensor detected 0.55 μg (0.033 mU) of recombinant MMP14 activity. Whilst, MT1-MMP serum levels are elevated in breast cancer patient samples (~0.017 ±0.006 μg/ml) [86], appropriate patient sample processing (e.g. protein concentration steps) would be required for the future use of AL-PHA MMP14 beads in breast cancer biomarker research studies.

However, in the case of membrane associated metalloproteinases (e.g. MT-MMPs and ADAMs), one potential strategy for concentrating samples could be the isolation of extracellular vesicles (EVs). Several types of EVs have been described and include exosomes, microvesicles, ectosomes, oncosomes and apoptotic bodies [87]. EVs are highly heterogeneous and differ in terms of their biogenesis, size (~30-1000 nm) and molecular compositions (lipid bilayers, ncRNAs, proteins and small molecules) [87]. EVs, including exosomes are readily accessible from patient liquid biopsies and recent studies indicate that EV-associated metalloproteinases have complex roles in cancer metastasis [87–89]. Lung cancer is a leading cause of cancer-related deaths and early detection could positively impact patient outcomes [90]. Importantly, within the context of lung cancer, the detection of ADAM10 proteolytic activity might be a more informative disease biomarker than *ADAM10* gene expression levels [35]. Indeed, exosomes isolated from *in vitro* models of lung cancer (e.g. A549 cells) or the

blood of non-small cell lung cancer (nsclc) patients exhibit increased ADAM10 activity [35,91]. Therefore, an ADAM10 specific AL-PHA biosensor may be a useful tool for lung cancer biomarker research. We thus tested the ability of an ADAM10-specific AL-PHA biosensor to detect for ADAM10 proteolytic activity (Fig. 6).

Prior to the commencement of AL-PHA biosensor assays, A549 EVs were characterised using nanoparticle tracking analyses (EV mode diameter 88.8 ±4.8 nm; Supplementary Fig. 9), Exo-Check dot blot array (CD81, CD63, ICAM, ANXA5, TSG101 positive; Supplementary Fig. 10), and flow cytometry surface marker characterisation (CD9, CD63 and CD81 positive; Supplementary Fig. 11). Previous studies have shown that A549 cells strongly express ADAM10 and ADAM10 is secreted within A549 extracellular vesicles [91,92]. Control and ADAM10-specific AL-PHA beads were treated with either 0 μg or 50 μg (total protein) of EVs, that were derived from an *in vitro* model (A549 cells) of non-small cell lung cancer. An EDTA-free protease inhibitor cocktail was also added to inhibit a broad array of serine and cysteine proteases but not metalloproteinases (see materials and methods).

ADAM10 AL-PHA and control assays were incubated at 37°C for 4 h and then analysed, post-assay, using plate reader and flow cytometry workflows (Fig. 6A). Relative supernatant fluorescence levels increased by 0.46 ±0.13-fold (~46% increase) for A549 EV-treated (50 μg) AL-PHA ADAM10 beads, compared against untreated control samples (0 μg) (Fig. 6B). Furthermore, A549 EV treatment (50 μg) also caused a significant decrease in AL-PHA bead fluorescence (-0.16 ±0.05 [~16% decrease]), whilst control beads and supernatant fluorescence levels were unaffected (Fig. 6B). Taken together, these data indicate positive detection of ADAM10 proteolytic activity and are in agreement with a previous study, that detected EV-associated ADAM10 proteolytic activity within 60 μg (total protein) of lysed nsclc-patient EVs

[35]. We envision that AL-PHA assays may enable a more simplified approach for detection. Future studies will be required to investigate if ADAM10 AL-PHA bead assays are sensitive enough to detect EV-associated ADAM10 within liquid biopsy samples or isolated patient exosomes. An advantage of AL-PHA beads is that, if required, their sensitivities can be boosted by optimising the linker lengths (Fig. 2), the proteolytic recognition motif or the reporter protein.

In order to optimise AL-PHA biosensor screening efficiency, we devised and tested a simple, semi high-throughput assay for screening AL-PHA metalloproteinase biosensor libraries (Fig. 7). Briefly, this assay was utilised to screen a panel of ten AL-PHA metalloproteinase biosensors, within a 96-well plate format, using human embryonic kidney 293 (HEK293) cell conditioned media. HEK293 cells are an industrially important mammalian cell line that have been previously used to manufacture therapeutic antibodies, recombinant proteins and extracellular vesicles [93,94]. Furthermore, HEK293 cells secrete MMPs including: MMP-9, -13,-14, ADAM -8, -10, -12, ADAMTS-1 and -5 [95–98]. To prepare conditioned media batches, HEK293 cells were cultured at a high cell density within a hollow fibre bioreactor (see materials and methods). The hollow fibre bioreactor was configured with a 20 kDa molecular weight cut off cartridge that essentially concentrated HEK293 cells (up to ~10^9 cells) and their secretomes (>20 kDa proteins and EVs) within ~20 ml harvest volumes. It should be noted that these cells were cultured using serum-free, Fluorobrite DMEM media so that there would be no calf-serum EVs or calf-serum-related proteolytic activity and also to reduce media background fluorescence-levels (e.g. phenol red) that might reduce downstream AL-PHA assay sensitivity. Control, TEV and metalloproteinase-specific AL-PHA beads were treated with 100 µl of either HEK293 cell conditioned media or unconditioned media (fresh Fluorobrite DMEM) within a 96-well plate assay format. The AL-PHA assay plate was

incubated within a plate reader (BMG, CLARIOstar) at 37ºC with shaking (300 rpm) for 4h and then analysed, post-assay, using plate reader and flow cytometry workflows (Fig. 7A). The general AL-PHA bead assay principle is unchanged, such that positive detection is evaluated in terms of an increase in supernatant fluorescence and a concomitant decrease in AL-PHA bead fluorescence. As expected, supernatant and AL-PHA bead fluorescence levels did not change for control and TEV AL-PHA biosensor samples (Fig. 7B, Supplementary Table 5). MMP9 proteolytic activity was also not detected (Fig. 7B, Supplementary Table 5). Though, positive detections were recorded for MMP-13, MMP-14, ADAM-8, ADAM-10, ADAM-12, ADAMTS-1 and ADAMTS-5 proteolytic activity within HEK293 cell conditioned media samples (Fig. 7B, Supplementary Table 5).

Interestingly, the flow cytometry and plate reader analyses differ in terms of their resultant AL-PHA biosensor detection sensitivities. This is perhaps not surprising given that there are fundamental differences (e.g. background fluorescence) between AL-PHA assay samples (e.g. conditioned cell media or protease assay buffers) and AL-PHA beads themselves. Likewise, there are clear technical differences between visual (transluminator), plate reader or flow cytometry illumination strengths (e.g. laser power), filters and detectors (e.g. photomultiplier tube [PMT] sensitivities). Generally, supernatant analyses (plate reader) provided more sensitive detection than AL-PHA bead analyses (flow cytometry). Indeed, the supernatant analyses indicated statistically significant positive detection for six different metalloproteinases, whilst flow cytometry analyses of AL-PHA beads detected activity from two metalloproteinases (Fig. 7B, Supplementary Table 5), Supernatant analyses also provided a more sensitive detection of AcTEV proteolytic activity (0.5 U) than AL-PHA bead analyses (1 U) (Fig. 3B). Whilst, visual assessments of AL-PHA beads should largely be reserved for highly active proteases (Supplementary Fig. 3, 6 and 7). However, whilst these plate reader,

flow cytometry and visual analyses slightly differ, they all fundamentally enable assessment of AL-PHA biosensors and the proteolytic activities that they are designed to detect. Beneficially, these different measurement approaches (visual, plate reader and flow cytometry) provide some flexibility in terms of the different contexts where AL-PHA biosensors can be implemented (e.g. diagnostic labs or in the field/point-of-care). Indeed, different AL-PHA biosensor applications may have different requirements for assay sensitivities (e.g. YES/NO detection vs. quantified protease activities) and readout formats (e.g. visual check or relative/absolute measurements). As such, this semi-high throughput AL-PHA biosensor screening strategy could conceivably be used to rapidly test future AL-PHA biosensor design optimisations and provide the necessary data to indicate whether single (e.g. visual, plate reader, flow cytometry) or combinatorial measurement strategies are required to ensure robust protease detection for any given downstream application.

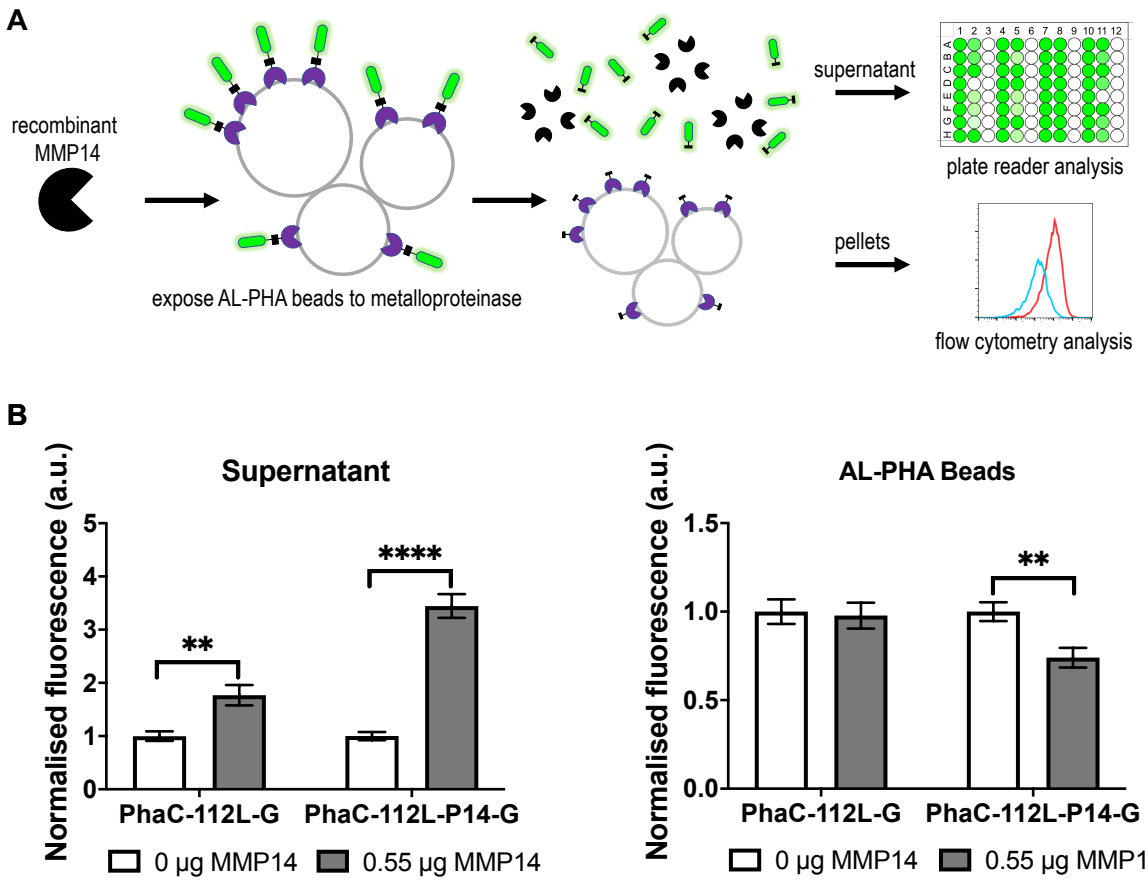

Figure 5 Detection of recombinant MMP14. (A) Matrix metalloproteinase 14 (MMP14) AL-PHA biosensor assay. **(B)** AL-PHA MMP14 (PhaC-112L-P14-G) and control (PhaC-112L-G) biosensors were treated with 0 µg or 0.55 µg of activated, recombinant MMP14. Supernatant fluorescence data (483-14 nm/530-30nm) of MMP14 treated AL-PHA biosensors were normalised against untreated controls of the same biosensor batch. AL-PHA beads were analysed using flow cytometry and the geometric mean (BL1-A, 488nm/530-30nm) of MMP14 treated AL-PHA biosensor beads were normalised against untreated controls of the same biosensor batch. Error bars denote standard error of the mean, n=8 (4 AL-PHA batches tested in duplicate), Student *t*-test **P<0.01 and ****P<0.0001.

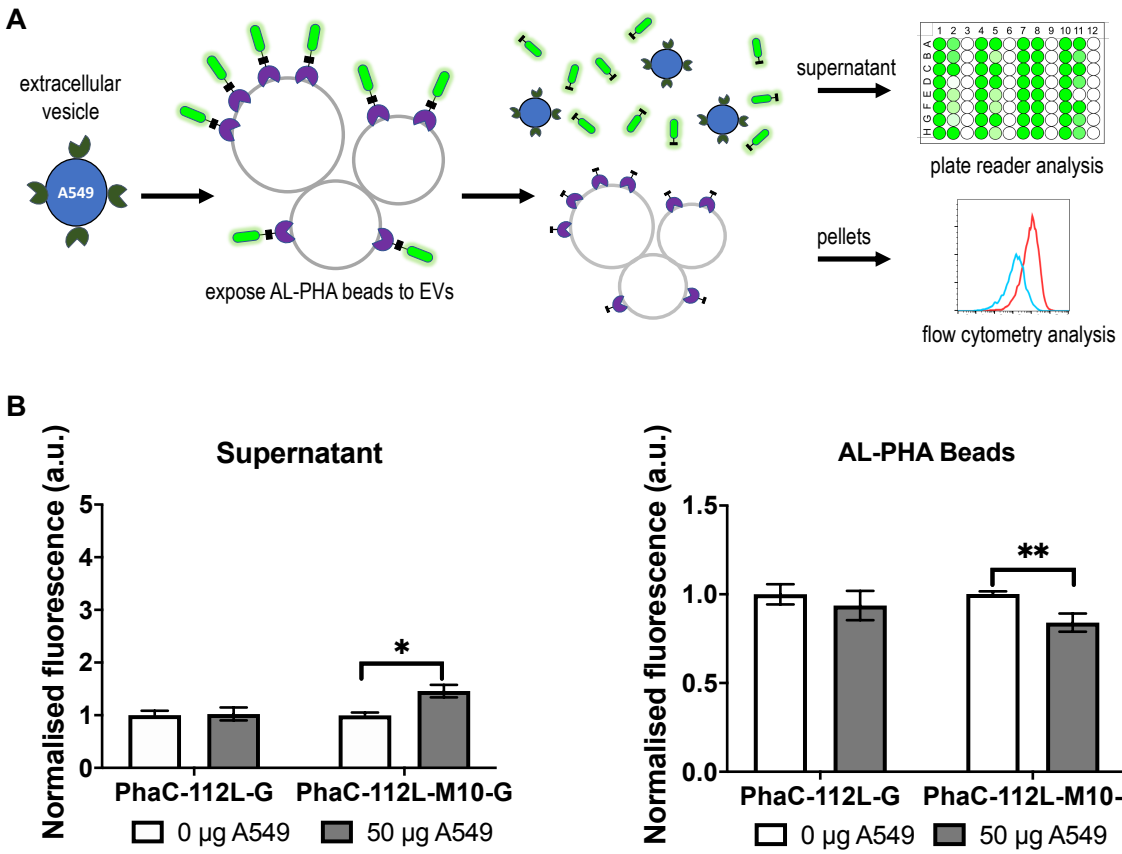

Figure 6 Detection of ADAM10 in A549 extracellular vesicles. (A) Extracellular vesicle (EV) AL-PHA biosensor assay. **(B)** AL-PHA biosensors were treated with 0 µg or 50 µg (total protein) of A549, non-small cell lung cancer cell line, extracellular vesicles. Supernatant fluorescence data (483-14 nm/530-30nm) of A549 EV treated AL-PHA biosensors were normalised against untreated controls of the same biosensor batch. AL-PHA beads were analysed using flow cytometry and the geometric mean (BL1-A, 488nm/530-30nm) of A549 EV treated AL-PHA biosensor beads were normalised against untreated controls of the same biosensor batch. Error bars denote standard error of the mean, n=4 (AL-PHA batches), Student *t*-test *P<0.05 and **P<0.01.

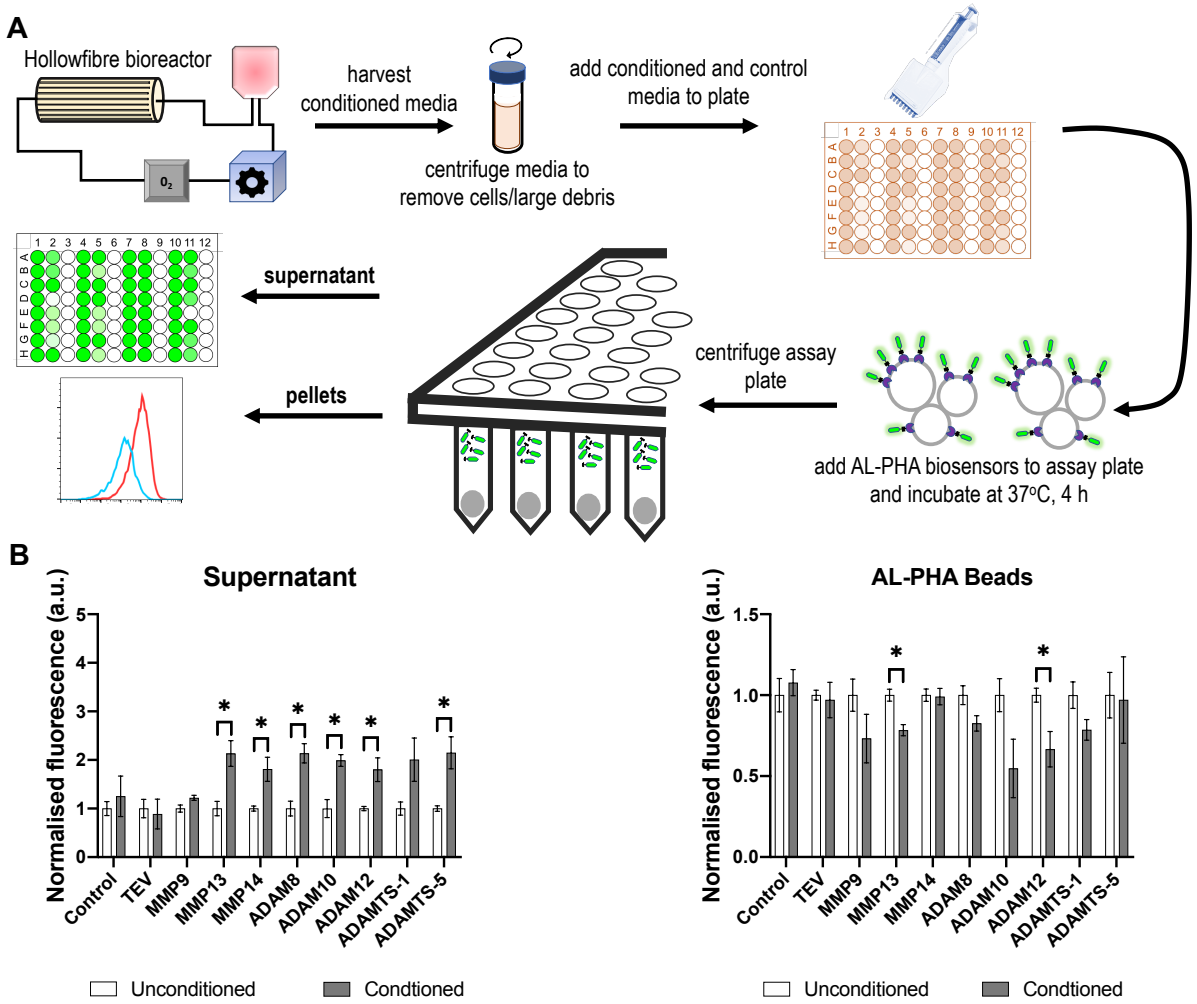

Figure 7 High-throughput metalloproteinase AL-PHA biosensor screening assay (A) HEK293 cells were cultured to a high cell density in a hollow fibre bioreactor. Cell conditioned media were assayed in 96-well plates against a panel of control and metalloproteinase AL-PHA biosensors. **(B)** AL-PHA biosensors were treated with either conditioned or unconditioned cell culture media. Supernatant fluorescence data (483-14 nm/530-30nm) of conditioned media treated AL-PHA biosensors were normalised against unconditioned media controls of the same biosensor batch. AL-PHA beads were analysed using flow cytometry and the geometric mean (BL1-A, 488nm/530-30nm) of conditioned media treated AL-PHA biosensor beads were normalised against unconditioned media controls of the same biosensor batch. Error bars denote standard error of the mean, n=3 (AL-PHA batches), Student *t*-test *P<0.05.

Conclusion

Protease structure-function studies continue to highlight the biomedical importance of proteases in an array of communicable and non-communicable diseases [14,99,100]. Beyond the exemplars within cancer (e.g. metalloproteinases) and parasitic diseases (e.g. cercarial elastase and schistosomiasis), proteases are also increasingly recognised for their roles within the progression of viral diseases [101]. Most recently, the main protease (M^{pro}/$3CL^{pro}$) of SARS-CoV-2, the causative virus of COVID-19 disease, is receiving global attention and ongoing research is exploring the rapid development of anti-coronaviral drugs that inhibit SARS-CoV-2 protease activity [102]. Naturally, protease activity assays can support these efforts [103,104]. Protease research is also important to a broad array of global health, bioremediation and industrial applications [39,105]. Therefore, novel strategies for detecting proteolytic activity are desirable. In response, biotechnological innovations have led to the development of an array of technologies that help address the evolving needs of protease research applications. Classical protease activity assays typically incorporate fluorogenic small molecule, peptide or nanoparticle substrates, Fluorescence Resonance Energy Transfer (FRET)-probes, electrochemical components or zymography methods [106–109]. Whereas, recent synthetic biology approaches have led to the development of more sophisticated modelling-led design strategies, the embedding of protease biosensors within smart materials and also increasingly complex whole-cell bioreporters [3,11–13,37].

Importantly, beyond the present study, several recent examples in the literature have also successfully demonstrated that specific protease activities can be detected from complex mixtures and biological samples [3,11,35,38]. Of course, protease biosensor implementations, especially those intended for field or point-of-care use, must consider these technical requirements (e.g. sensitivity and specificity) alongside any relevant responsible research and innovation requirements (e.g. implementation costs as well as political, regulatory and societal

contexts) [3]. These classical and synthetic biology approaches each have their own advantages and limitations, several of which we briefly summarise and compare alongside AL-PHA beads (Table 1).

Primarily, AL-PHA beads were designed to be highly modular such that each of the fusion protein elements can be easily customised or optimised for different global health applications, measurement approaches (visual or instrumental) and settings (e.g. laboratory or field use). For example, the protease recognition motifs are interchangeable and can be altered to improve specificity towards proteases of interest. Likewise, the reporter protein (sfGFP) could also be changed, for example, to red fluorescent protein or β-galactosidase in line with cultural sensitivities around reporter colour [3], or as an additional means to optimise AL-PHA biosensor sensitivity. Beneficially, AL-PHA beads are also non-living and are biodegradable [110]. Indeed, their degradation can be readily accelerated, if required, through enzymatic means (e.g. PhaZ enzyme) [59] which further extends the flexibility of their implementation and safe disposal. We also estimate that the raw material cost to microbially produce enough AL-PHA beads for a typical AL-PHA assay, is around 2-4 pence (GBP). Even when sample processing costs, labour and other miscellaneous costs are taken into account, AL-PHA assays are likely to remain cost competitive against competing technologies.

In conclusion, AL-PHA beads are a library of low-cost, biodegradable, bioplastic-based protease biosensors that can be applied to global health applications. In the longer term, we envision that AL-PHA bead biosensors will lead to the development of low-cost global health biosensors for use in resource-limited settings.

Table 1. Comparative advantages and disadvantages of AL-PHA beads

	AL-PHA beads	Small molecule substrates	Peptides	Quantum dots	FRET-probes	Whole-cell bioreporters
Modular Design	√√√	√	√√	√	√√√	√√√
Development time-scale	Several days	Several weeks	Several days or weeks	Several weeks	Several days	Several days
Assay flexibility	√√√	√√√	√√√	√√	√√√	√
Producible within a standard molecular laboratory	YES	POSSIBLY	POSSIBLY	NO	YES	YES
Shelf-life	√√√	√√√	√√	√	√√	√√
Regulated GMO	No	No	No	No	No	Potentially
Production cost	£	£	££	£££	££	£
Environmentally friendly	√√√	√	√√√	√	√√√	√√

Materials and methods

Bacterial strains and general growth conditions

Plasmid constructs and strains used in this study are listed in Supplementary Table 3. *E. coli* JM109 was used for both cloning and production of AL-PHA protease biosensors. For plasmid recovery *E. coli* strains were grown in Luria-Bertani (LB) medium supplemented with 34 μg/ml Chloramphenicol (final concentration) and cultured at 37°C with shaking (220 rpm). During PHAs and AL-PHA bead production *E. coli* strains were grown in Terrific-Broth (TB) supplemented with 34 μg/ml Chloramphenicol (final concentration) and 3% glucose (w/v), cultured at 37°C with shaking (220 rpm).

Construct assembly

Empty vector plasmid EV104 was originally sourced from the 2013 distribution of the iGEM Registry of Standard Biological Parts (partsregistry.org; BBa_K608002) and was transformed during this study into *E. coli* JM109 to create strain EV104-JM109. Plasmid C104-JM109, encoding a constitutively expressed, engineered *phaCAB* operon was originally derived from our previous study [59] and was transformed during this study into *E. coli* JM109 to create strain C104-JM109. C104-JM109 was used to create wild-type, non-functionalised PHAs beads.

For first generation AL-PHA biosensor construction, the PhaC fusion (12L-G) region was ordered as a dsDNA gene synthesis fragment (GeneArt String, ThermoFisher, USA) and primer pair RK028/RK029 were used to amplify and linearise plasmid C104-JM109. In-Fusion cloning (Takara Bio, USA) of linearised C104-JM109 with the GeneArt String and transformation into *E. coli* JM109 was used to clone the first-generation AL-PHA biosensor

control plasmid (PhaC-12L-G; pYZW1). In order to incorporate protease recognition motifs (TEV, MMP, ADAM and ADAMTS) into the linker region, plasmid pYZW1 was used as a PCR template with appropriate primer pairs (YZW11-YZW78). The resultant PCR products were digested with *Dpn*I, phosphorylated, re-ligated and transformed into *E. coli* JM109, resulting in plasmids/strains pYZW2- pYZW29.

For second generation AL-PHA biosensor construction, the longer flexible amino acid linker (22L) region was incorporated using PCR. Briefly, first generation AL-PHA biosensor plasmids were used as templates in PCR reactions, along with primer pair YZW81/YZW82. The resultant PCR products were digested with *Dpn*I, phosphorylated, re-ligated and transformed into *E. coli* JM109, resulting in the second-generation biosensor plasmids/strains PhaC-22L-G (pYZW33) and PhaC-22L-T-G (pYZW34).

For third generation AL-PHA biosensor construction, the longer flexible amino acid linker (112L) region was ordered as a dsDNA gene synthesis fragment (gBlock, IDT, USA) and primer pair YZW83/YZW84 was used to amplify and linearise all first-generation AL-PHA biosensor plasmids. In-Fusion cloning (Takara Bio, USA) of linearised first-generation AL-PHA biosensor plasmids with the gBlock and subsequent transformation into *E. coli* JM109 resulted in the third-generation AL-PHA biosensor constructs/strains (pYZW39-pYZW48). The third-generation Elastase biosensor (PhaC-112L-E-G) was cloned separately. Briefly, plasmid pYZW40 (PhaC-112L-T-G) was used as a PCR template, along with primer pair AJW671/AJW672. The resultant PCR products were digested with *Dpn*I, phosphorylated, re-ligated and transformed into *E. coli* JM109, resulting in third-generation Elastase biosensor plasmid/strain PhaC-112L-E-G (pAJW290).

Oligonucleotide primers used for generating biosensor constructs and DNA sequencing are shown in Supplementary Table 4.

Production, and characterisation of AL-PHA biosensor beads

Glycerol stocks of control (C104-JM109) or AL-PHA biosensor strains were used to inoculate flasks containing 100 ml Terrific Broth (TB), supplemented with 3% glucose (w/v) and 34 μg/ml Chloramphenicol (Cam). These production cultures were incubated at 37°C with shaking at 200 rpm for 24 h. Subsequently, these production cultures were harvested via centrifugation at 3220 *g* for 10 minutes at 4°C. The resultant cell pellets were washed twice in phosphate-buffered saline (PBS) (1X), before being re-suspended into 1 ml PBS (1X) per gram of the cell pellet and transferred into 2 ml microtubes. To release PHAs/AL-PHA biosensor beads, samples were sonicated using a Vibra-cell VCX130 sonicator (SONICS, Newtown, USA), with a 6 mm diameter probe, on ice (3 × 40 s with 59 s cooling interval; output frequency: 20 kHz; amplitude: 50 %). Post-lysis, samples were centrifuged 6000 *g* for 10 minutes at 4°C and then gently re-suspended (5 seconds at setting 5) using a vortex machine (Heidolph, REAX 2000). Samples were sonicated a second time (2 × 20 s with 59 s cooling interval; output frequency: 20 kHz; amplitude: 50 %) on ice and then centrifuged 6000 *g* for 10 minutes at 4°C. The supernatant was removed and the released PHAs/AL-PHA beads were re-suspended as a 20 % slurry (pellet w/v in PBS). PHAs/AL-PHA bead batches were stored at 4°C with 2 μl kanamycin (stock concentration 25 μg/ml) per microtube batch to prevent bacterial growth. PHAs and AL-PHA biosensor beads were analysed using dynamic light scattering (DLS) on a Malvern Zetasizer Nano ZS (Malvern Instruments, Malvern, UK). Harvested PHAs/AL-PHA biosensor beads were diluted 100-fold into PBS (1X) and at least three technical replicates per sample were measured at 25°C.

SmCTF sample preparation

The three SmCTF samples tested (SmCTF1-3) were produced by BioGlab Ltd. (Nottingham, UK) as previously described [11,70]. Freeze-dried SmCTF samples were reconstituted in sterile distilled water and stored at -20°C until required.

MMP14 activation reactions

Recombinant human MMP-14 (MT1-MMP) metalloproteinase (ab#168081, Abcam, MA, USA) was commercially sourced and activated according to the manufacturer's instructions. Briefly, MMP14 activation reactions were 100 µl in total and consisted of 25 µl MMP14 (5 µg), 1 µl of 50 µg TPCK-trypsin per ml activation buffer (#T1426-50MG, Sigma-Aldrich, MO, USA) and 74 µl of activation buffer (50mM TRIS-HCl, pH 7.5, 150 mM NaCl, 5 mM $CaCl_2$). Activation reactions were incubated at 25°C for 12 min. Post-incubation, 1 µl of 1 mg/ml aprotinin (activation buffer; #Ab146286, Abcam MA, USA) was added to inactivate TPCK-trypsin.

Hollow fibre cell culture

HEK293 cells were cultured at a high cell density using a hollow fibre bioreactor (FiberCell Systems, Inc., MD, USA), which was configured with a 20 kDa molecular weight cut off cartridge (#C2011, FiberCell Systems, Inc., MD, USA) that essentially concentrated HEK293 cells (up to ~10^9 cells) and their secretomes (>20 kDa proteins and EVs) within ~20 ml cartridge/harvest volumes. The hollow fibre cartridge was sequentially primed, pre-culture by PBS (1X; #14190144, ThermoFisher Scientific, MA, USA), serum-free Fluorobrite DMEM (

#A1896702, ThermoFisher Scientific, MA, USA) and Fluorobrite DMEM (#A1896702, ThermoFisher Scientific, MA, USA) supplemented with 10% Exosome-Depleted Fetal Bovine Serum (FBS, #A25904DG, ThermoFisher Scientific, MA, USA), each for 24 h. Once primed, $1x10^8$ adherent HEK293 cells were seeded into the cartridge. HEK293 cell line validation was carried out by Eurofins (Supplementary Fig. 12). Cell growth rate was indirectly evaluated through daily monitoring of the glucose level of the cell culture medium (#GC001000, FiberCell Systems, Inc., MD, USA). The cell culture medium was changed once glucose levels significantly decreased to less than half the original level. Once glucose consumption levels significantly increased (e.g. 50% glucose consumed within 24 h) the cell culture media was changed to Fluorobrite DMEM (#A1896702, ThermoFisher Scientific, MA, USA) supplemented with 10% Chemically Defined Medium for High Density Cell Culture (#CDM HD, FiberCell Systems, Inc., MD, USA), a protein-free FBS replacement. Samples (~ 20 ml volume) were harvested from the hollow fibre cartridge each day and HEK293 cells were cultured for a week, using serum free media prior to harvesting conditioned media for AL-PHA assays.

AL-PHA biosensor assays

AL-PHA biosensor reactions were setup according to the optimal activity requirements of the proteases being detected. Trypsin AL-PHA assays: 50 µl (total volume) reactions were setup within 1.5ml microtubes and included the following components: 1 µl of purified AL-PHA beads (PhaC-22L-G), 0 or 1 µg Sequencing Grade Modified Trypsin (0 or 10 µl; #V5111, Promega, WI, USA) that was reconstituted within trypsin re-suspension buffer (50 mM acetic acid; #V542A, Promega, WI, USA), and 39 µl or 49 µl 250 mM Tris buffer. These reactions were incubated for 2 h at 37^{o}C with 220 rpm shaking (Eppendorf, Thermo Mixer C). AcTEV

protease AL-PHA assays: 100 µl (total volume) reactions were setup within 1.5 ml microtubes and included the following components: 1 µl of purified AL-PHA beads, 0-10 U AcTEV (0-1 µl; #12575015, ThermoFisher Scientific, MA, USA), 1 µl of dithiothreitol (DTT) 0.1M, 5 µl of TEV reaction buffer (20X; 1M Trix-HCl pH8.0, 10mM EDTA), and 92-93 µl of PBS (1X). These reactions were incubated for 0-6 h at 30°C with 500 rpm shaking (Eppendorf, Thermo Mixer C). *S. mansoni* cercarial elastase AL-PHA assays: 100 µl (total volume) reactions were setup within 1.5 ml microtubes and included the following components, 1 µl of purified AL-PHA beads, 10 µl of reconstituted SmCTF sample and 89 µl PBS (1X). These reactions were incubated for 2 h at 30°C with 500 rpm shaking (Eppendorf, Thermo Mixer C). MMP14 AL-PHA assays: 100 µl (total volume) reactions were setup within 1.5ml microtubes and included the following components, 1 µl of purified AL-PHA beads, 0 or 0.55 µg of activated MMP14 (0 or 11 µl), 87 or 98 µl of activation buffer (50mM TRIS-HCl, pH 7.5, 150 mM NaCl, 5 mM $CaCl_2$) and 1µl of 1 mg/ml aprotinin (activation buffer; #Ab146286, Abcam MA, USA). These reactions were incubated for 4 h at 37°C with 500 rpm shaking (Eppendorf, Thermo Mixer C). EV-associated ADAM10 AL-PHA assays: 100 µl (total volume) reactions were setup within 1.5 ml microtubes and included the following components, 1 µl of purified AL-PHA beads, 0 or 50 µg of A549 EVs (0 or 50 µl; #HBM-A549-100/5, HansaBioMed, Tallinn, Estonia), 4 µl of cOmplete™ EDTA-free protease inhibitor cocktail (50X; #11873580001, Sigma-Aldrich, MO, USA) and 45 µl or 95 µl PBS (1X). These reactions were incubated for 4 h at 37°C with 500 rpm shaking (Eppendorf, Thermo Mixer C). HEK293 conditioned media AL-PHA assays: 100 µl (total volume) reactions were setup within the wells of a 96-well plate (#655076, Greiner Bio-One, Kremsmünster, Austria) and included the following components, 0 or 1 µl of purified control (C104) PHAs beads, 0 µl or 1 µl of purified AL-PHA beads, 0 or 99 µl of fresh, serum-free non-conditioned media (Fluorobrite DMEM; #A1896702, ThermoFisher Scientific, MA, USA) and 0 or 99 µl of HEK293 conditioned cell media (see hollow fibre cell culture materials

and methods section). These 96-well assay plates were incubated for 4 h, within a plate reader (CLARIOstar, BMG, Ortenberg, Germany) at 37^{o}C with 300 rpm shaking.

Post-incubation, AL-PHA assay tubes were centrifuged ≥6000 *g* for 10 minutes, whilst AL-PHA assay plates were centrifuged 500 *g* for 10 minutes (MPS 1000 Mini PCR Plate Spinner, Sigma-Aldrich, MO, USA) in order to pellet AL-PHA beads. Post-centrifugation, 20 µl of each AL-PHA assay supernatant were separately sampled and transferred to a black, µClear 384 well plate (#781096, Greiner Bio-One, Kremsmünster, Austria) for plate reader analyses (Excitation 483-14 nm/Emission 530-30; CLARIOstar, BMG, Ortenberg, Germany). Supernatant fluorescence measurements of protease treated AL-PHA biosensors were normalised against non-treated controls of the same biosensor batch. Whilst, pelleted AL-PHA beads were re-suspended into 1 ml PBS (1X) and around 10,000 events for each sample were analysed using flow cytometry (Attune NxT, ThermoFisher Scientific, MA, USA). The geometric mean (BL1-A, Excitation 488 nm/Emission 530/30 nm) of protease treated AL-PHA beads were normalised against non-treated controls of the same biosensor batch and at least three batches of each AL-PHA biosensor were tested in all AL-PHA assays. The flow cytometry gating strategy used (Supplementary Fig. 4) was also validated with the assistance of 1 µm bead standards (#F13839, Thermo Fisher Scientific, MA, USA).

GFP Calibration curve

Super folder green fluorescent protein (sfGFP) samples were purified from AL-PHA beads and used to create an AL-PHA GFP calibration curve (Supplementary Fig. 5). Briefly, four 1.5 ml microtubes were setup with 4 µl of purified AL-PHA beads (PhaC-112L-T-G) and 96 µl PBS (1X). These samples were centrifuged (6000 *g* for 10 minutes) to wash and pellet the AL-PHA

beads and post-centrifugation the supernatant was carefully removed. AL-PHA beads were then re-suspended within 100 µl (total volume) of AcTEV reaction solutions that included the following components: 4 µl of re-suspended AL-PHA beads (PhaC-112L-T-G), 20 U AcTEV (2 µl; #12575015, ThermoFisher Scientific, MA, USA), 1 µl of dithiothreitol (DTT) 0.1M, 5 µl of TEV reaction buffer (20X; 1M Trix-HCl pH8.0, 10mM EDTA), and 88 µl of PBS (1X). These reactions were incubated for 3 h at 30ºC with 500 rpm shaking (Thermo Mixer C, Eppendorf, Germany). Post-incubation, these reactions were centrifuged 6000 *g* for 10 minutes to pellet the AL-PHA beads. Supernatants containing proteolytically released sfGFP were combined and concentrated at 45ºC for 20 min with VAQ setting, using an Eppendorf concentrator (Eppendorf, Germany). The protein concentration of purified sfGFP samples was determined, according to the manufactures' guidance, using a Qubit 3 Fluorometer (Thermo Fisher Scientific, MA, USA) and a Qubit Protein Assay Kit (#Q33211, Thermo Fisher Scientific, MA, USA). The sfGFP purification samples were combined and analysed via sodium dodecyl sulphate (SDS)-polyacrylamide gel electrophoresis (PAGE) using 4–12% Bis-Tris gels (NuPAGE Novex, Thermo Fisher Scientific, MA, USA), followed by western blot analysis using a HRP-conjugated GFP-specific polyclonal antibody (1:4,000 dilution; #A10260, Thermo Fisher Scientific, MA, USA). Western blots were developed by enhanced chemiluminence (ECL). Additionally, the combined sfGFP purification sample was used to setup a GFP calibration curve. Calibration samples for each sfGFP concentration were setup in quadruplicate then aliquoted into 384-well plates (#781096, Greiner Bio-One, Kremsmünster, Austria) and measured using a CLARIOstar plate reader (Excitation 483-14 nm/Emission 530-30; BMG, Ortenberg, Germany).

Extracellular vesicle characterisation

Nanoparticle tracking analysis (NTA): 1 µL A549 EVs (1 mg/ml; #HBM-A549-100/5, HansaBioMed, Tallinn, Estonia) were diluted (1:1000) within particle-free DPBS (1X; #14190144, Thermo Fisher Scientific), gently pipetted for 10 s and then aliquoted into a deep-well, 96-well plate. Samples from the 96-well plate were injected into a NanoSight NS300 NTA instrument equipped with a NanoSight Sample Assistant (Malvern Instruments, UK) autosampler system. The NTA images were recorded and analysed to obtain the concentration and distribution of the sample particles. Additional software version and measurement settings are shown in supplementary figure 9. Exo-Check Array: A549 protein markers were characterised using a commercially sourced Exo-Check Exosome Antibody Array kit (#EXORAY200A-4, System Biosciences, CA, USA). A549 EVs (100 µg; #HBM-A549-100/5, HansaBioMed, Tallinn, Estonia) were lysed and processed according to the manufacturer's guidelines and the developed dot blot array was imaged using a ChemiDoc imaging system (Bio-Rad Laboratories Inc., USA) (Supplementary Fig. 10). Flow cytometry analysis of EV surface markers: Several A549 EV samples were setup and included the following components: 25 µl of A549 EVs (25 µg; #HBM-A549-100/5, HansaBioMed, Tallinn, Estonia) were incubated with 20 µl of Exosome-Human CD63 Dynabeads (#10606D, Thermo Fisher Scientific, MA, USA) and 53 µl of DPBS (1X; #14190144, Thermo Fisher Scientific) at 25^{o}C for 1 hour with shaking 1000 rpm (Thermo Mixer C, Eppendorf, Germany) in order to bind CD63+ EVs. Post-incubation, samples were transferred to a magnetic rack and unbound EVs were washed away using DPBS (1X). Dynabead-EV samples were re-suspended into 98 µl DPBS and 2 µl of one of the following antibodies: IgG1-PE (#130-113-200, Miltenyi Biotec, Germany), CD9-PE, human (#130-103-955, Miltenyi Biotec, Germany), CD63-PE, human (#130-100-153, Miltenyi Biotec, Germany) or CD81-PE, human (#130-118-342, Miltenyi Biotec, Germany). Samples were subsequently incubated at 25^{o}C for 1 hour with shaking 1000 rpm (Thermo Mixer C, Eppendorf, Germany) in order to fluorescently label EVs. Post-

incubation, samples were transferred to a magnetic rack and unbound antibodies were washed away using DPBS (1X). Dynabead-EV samples were then re-suspended into 500 µl DPBS and analysed using flow cytometry (Attune NxT, ThermoFisher Scientific, MA, USA; YL1-A Excitation 561 nm/Emission 585-16 nm).

Statistics

Statistical analysis (standard error of the mean, s.e.m and unpaired t-test) was carried out on at least three experimental replicates using GraphPad Prism 8.4.2 (GraphPad Software Inc., La Jolla, California) and flow cytometry data analysis was performed using FlowJo (vX 10.5.3) software.

Declaration of conflicts of interest

The authors declare that the research was conducted in the absence of any commercial or financial relationships that could be construed as a potential conflict of interest.

Acknowledgements

Dr Richard Kelwick is supported by the Cancer Research UK Imperial Centre Development Fund and until recently, was supported by a BBSRC-funded Royal Society of Edinburgh Enterprise Fellowship. Dr Alexander Webb, Dr Fiona Allan, Dr Aidan Emery, Prof. Michael Templeton and Prof. Paul Freemont are supported by the UK Government's Global Challenges Research Fund (GCRF) through the EPSRC grant [EP/P028519/1], as part of the WISER project. We also acknowledge the support of Imperial Confidence in Concept (MRC/EPSRC), Imperial College London EPSRC Impact Acceleration Account [EP/R511547/1], EPSRC grant

[EP/L011573/1], and BBSRC grant [BB/L027852/1]. We thank Prof. Michael Doenhoff for SmCTF samples. We also thank colleagues in the Section of Structural and Synthetic Biology, as well as Prof. Michael Seckl, Dr Roy Rajat, Dr David McClymont, and Prof. Dylan Edwards for their advice.

Supplementary Data

Supplementary data associated with this article can be found in the online version.

References

[1] R. Kelwick, J.T. MacDonald, A.J. Webb, P. Freemont, Front. Bioeng. Biotechnol. 2 (2014) 60.
[2] M. Hicks, T.T. Bachmann, B. Wang, ChemPhysChem 21 (2020) 132–144.
[3] A.J. Webb, R. Kelwick, P.S. Freemont, Microb. Biotechnol. 10 (2017) 244–249.
[4] W. Thavarajah, M.S. Verosloff, J.K. Jung, K.K. Alam, J.D. Miller, M.C. Jewett, S.L. Young, J.B. Lucks, Npj Clean Water 3 (2020) 18.
[5] X. Wan, F. Volpetti, E. Petrova, C. French, S.J. Maerkl, B. Wang, Nat. Chem. Biol. 15 (2019) 540–548.
[6] N. Ostrov, M. Jimenez, S. Billerbeck, J. Brisbois, J. Matragrano, A. Ager, V.W. Cornish, Sci. Adv. 3 (2017) e1603221.
[7] K.Y. Wen, L. Cameron, J. Chappell, K. Jensen, D.J. Bell, R. Kelwick, M. Kopniczky, J.C. Davies, A. Filloux, P.S. Freemont, ACS Synth. Biol. Accepted (2017) acssynbio.7b00219.
[8] N. Gupta, V. Renugopalakrishnan, D. Liepmann, R. Paulmurugan, B.D. Malhotra, Biosens. Bioelectron. 141 (2019) 111435.
[9] A.D. Silverman, A.S. Karim, M.C. Jewett, Nat. Rev. Genet. 21 (2020) 151–170.
[10] J.R. van der Meer, S. Belkin, Nat. Rev. Microbiol. 8 (2010) 511–522.
[11] A.J. Webb, R. Kelwick, M.J. Doenhoff, N. Kylilis, J.T. MacDonald, K.Y. Wen, C. McKeown, G. Baldwin, T. Ellis, K. Jensen, P.S. Freemont, Sci. Rep. 6 (2016) 24725.
[12] R.J.R. Kelwick, A.J. Webb, P.S. Freemont, Front. Bioeng. Biotechnol. 8 (2020).
[13] H.J. Wagner, R. Engesser, K. Ermes, C. Geraths, J. Timmer, W. Weber, Mater. Today 22 (2019) 25–34.
[14] J.S. Bond, J. Biol. Chem. 294 (2019) 1643–1651.
[15] M. Vizovišek, R. Vidmar, M. Drag, M. Fonović, G.S. Salvesen, B. Turk, Trends Biochem. Sci. 43 (2018) 829–844.
[16] C. López-Otín, J.S. Bond, J. Biol. Chem. 283 (2008) 30433–7.
[17] N. Levi, N. Papismadov, I. Solomonov, I. Sagi, V. Krizhanovsky, FEBS J. (2020) febs.15282.
[18] S. Freitas-Rodríguez, A.R. Folgueras, C. López-Otín, Biochim. Biophys. Acta - Mol. Cell Res. 1864 (2017) 2015–2025.
[19] R. Kelwick, I. Desanlis, G.N. Wheeler, D.R. Edwards, Genome Biol. 16 (2015) 113.

[20] C. Herrera, T. Escalante, A. Rucavado, J.W. Fox, J.M. Gutiérrez, Expert Rev. Proteomics 15 (2018) 967–982.
[21] H.W. Jackson, V. Defamie, P. Waterhouse, R. Khokha, Nat. Rev. Cancer 17 (2017) 38–53.
[22] J. Lambert, K. Makin, S. Akbareian, R. Johnson, A.A.A. Alghamdi, S.D. Robinson, D.R. Edwards, J. Cell Sci. 133 (2020) jcs235762.
[23] R. Kelwick, L. Wagstaff, J. Decock, C. Roghi, L.S. Cooley, S.D. Robinson, H. Arnold, J. Gavrilović, D.M. Jaworski, K. Yamamoto, H. Nagase, B. Seubert, A. Krüger, D.R. Edwards, Int. J. Cancer 136 (2015) E14–E26.
[24] V. Quesada, G.R. Ordonez, L.M. Sanchez, X.S. Puente, C. Lopez-Otin, Nucleic Acids Res. 37 (2009) D239–D243.
[25] S.S. Apte, W.C. Parks, Matrix Biol. 44–46 (2015) 1–6.
[26] M. Mullooly, P.M. McGowan, J. Crown, M.J. Duffy, Cancer Biol. Ther. 17 (2016) 870–880.
[27] G.W. Huntley, Nat. Rev. Neurosci. 13 (2012) 743–757.
[28] J.H. McKerrow, C. Caffrey, B. Kelly, P. Loke, M. Sajid, Annu. Rev. Pathol. Mech. Dis. 1 (2006) 497–536.
[29] D.P. McManus, D.W. Dunne, M. Sacko, J. Utzinger, B.J. Vennervald, X.-N. Zhou, Nat. Rev. Dis. Prim. 4 (2018) 13.
[30] P.J. Hotez, M. Alvarado, M.-G. Basáñez, I. Bolliger, R. Bourne, M. Boussinesq, S.J. Brooker, A.S. Brown, G. Buckle, C.M. Budke, H. Carabin, L.E. Coffeng, E.M. Fèvre, T. Fürst, Y.A. Halasa, R. Jasrasaria, N.E. Johns, J. Keiser, C.H. King, R. Lozano, M.E. Murdoch, S. O'Hanlon, S.D.S. Pion, R.L. Pullan, K.D. Ramaiah, T. Roberts, D.S. Shepard, J.L. Smith, W.A. Stolk, E.A. Undurraga, J. Utzinger, M. Wang, C.J.L. Murray, M. Naghavi, PLoS Negl. Trop. Dis. 8 (2014) e2865.
[31] WHO, World Heal. Organ. (2020).
[32] J.P. Salter, K.-C. Lim, E. Hansell, I. Hsieh, J.H. McKerrow, J. Biol. Chem. 275 (2000) 38667–38673.
[33] J.P. Salter, Y. Choe, H. Albrecht, C. Franklin, K.-C. Lim, C.S. Craik, J.H. McKerrow, J. Biol. Chem. 277 (2002) 24618–24624.
[34] S. Liu, Q. Zheng, Z. Wang, Bioinformatics (2020).
[35] T. Yoneyama, M. Gorry, A. Sobo-Vujanovic, Y. Lin, L. Vujanovic, A. Gaither-Davis, M.L. Moss, M.A. Miller, L.G. Griffith, D.A. Lauffenburger, L.P. Stabile, J. Herman, N.L. Vujanovic, J. Cancer 9 (2018) 2559–2570.
[36] A. Kirchhain, N. Poma, P. Salvo, L. Tedeschi, B. Melai, F. Vivaldi, A. Bonini, M. Franzini, L. Caponi, A. Tavanti, F. Di Francesco, TrAC Trends Anal. Chem. 110 (2019) 35–50.
[37] D.K. Agrawal, E.M. Dolan, N.E. Hernandez, K.M. Blacklock, S.D. Khare, E.D. Sontag, ACS Synth. Biol. 9 (2020) 198–208.
[38] A. Gräwe, J. Ranglack, W. Weber, V. Stein, Curr. Opin. Biotechnol. 63 (2020) 1–7.
[39] A. Razzaq, S. Shamsi, A. Ali, Q. Ali, M. Sajjad, A. Malik, M. Ashraf, Front. Bioeng. Biotechnol. 7 (2019).
[40] H.-E. Lai, C. Canavan, L. Cameron, S. Moore, M. Danchenko, T. Kuiken, Z. Sekeyová, P.S. Freemont, Trends Biotechnol. 37 (2019) 1146–1151.
[41] S. Slomovic, K. Pardee, J.J. Collins, Proc. Natl. Acad. Sci. 112 (2015) 14429–14435.
[42] P.G. Movizzo, W.C. Ruder, Z. Long, MethodsX 6 (2019) 1331–1335.
[43] D. Wolozny, J.R. Lake, P.G. Movizzo, Z. Long, W.C. Ruder, Engineering 5

(2019) 173–180.
[44] O. Wright, M. Delmans, G.-B. Stan, T. Ellis, ACS Synth. Biol. 4 (2015) 307–316.
[45] S.Y. Choi, I.J. Cho, Y. Lee, Y.-J. Kim, K.-J. Kim, S.Y. Lee, Adv. Mater. (2020) 1907138.
[46] B.H.A. Rehm, Nat. Rev. Microbiol. 8 (2010) 578–592.
[47] J.J. Koskimäki, M. Kajula, J. Hokkanen, E.-L. Ihantola, J.H. Kim, H. Hautajärvi, E. Hankala, M. Suokas, J. Pohjanen, O. Podolich, N. Kozyrovska, A. Turpeinen, M. Pääkkönen, S. Mattila, B.C. Campbell, A.M. Pirttilä, Nat. Chem. Biol. 12 (2016) 332–338.
[48] B. Laycock, P. Halley, S. Pratt, A. Werker, P. Lant, Prog. Polym. Sci. 38 (2013) 536–583.
[49] G.-Q. Chen, X.-R. Jiang, Curr. Opin. Biotechnol. 53 (2018) 20–25.
[50] R. Tarrahi, Z. Fathi, M.Ö. Seydibeyoğlu, E. Doustkhah, A. Khataee, Int. J. Biol. Macromol. 146 (2020) 596–619.
[51] M.F. Moradali, B.H.A. Rehm, Nat. Rev. Microbiol. 18 (2020) 195–210.
[52] Z.A. Raza, S. Riaz, I.M. Banat, Biotechnol. Prog. 34 (2018) 29–41.
[53] S.Y. Lee, Nat. Biotechnol. 24 (2006) 1227–1229.
[54] G.-Q. Chen, Chem. Soc. Rev. 38 (2009) 2434.
[55] J. Możejko-Ciesielska, R. Kiewisz, Microbiol. Res. 192 (2016) 271–282.
[56] G.-Q. Chen, Q. Wu, Biomaterials 26 (2005) 6565–6578.
[57] G.-Q. Chen, A.-C. Albertsson, Biomacromolecules 20 (2019) 3211–3212.
[58] S.Y. Lee, Y. Lee, Appl. Environ. Microbiol. 69 (2003) 3421–3426.
[59] R. Kelwick, M. Kopniczky, I. Bower, W. Chi, M.H.W. Chin, S. Fan, J. Pilcher, J. Strutt, A.J. Webb, K. Jensen, G.-B. Stan, R. Kitney, P. Freemont, PLoS One 10 (2015) e0117202.
[60] A. Hiroe, K. Tsuge, C.T. Nomura, M. Itaya, T. Tsuge, Appl. Environ. Microbiol. 78 (2012) 3177–3184.
[61] R. Kelwick, L. Ricci, S.M. Chee, D. Bell, A.J. Webb, P.S. Freemont, Synth. Biol. 3 (2018).
[62] T.M.M.M. Amaro, D. Rosa, G. Comi, L. Iacumin, Front. Microbiol. 10 (2019).
[63] B.T. Bäckström, J.A. Brockelbank, B.H.A. Rehm, BMC Biotechnol. 7 (2007) 3.
[64] J.X. Wong, M. Gonzalez-Miro, A.J. Sutherland-Smith, B.H.A. Rehm, Front. Bioeng. Biotechnol. 8 (2020).
[65] I.D. Hay, J. Du, P.R. Reyes, B.H.A. Rehm, Microb. Cell Fact. 14 (2015) 190.
[66] N.A. Parlane, D.N. Wedlock, B.M. Buddle, B.H.A. Rehm, Appl. Environ. Microbiol. 75 (2009) 7739–7744.
[67] J.L. Draper, B.H. Rehm, Bioengineered 3 (2012) 203–208.
[68] J. Tian, A. He, A.G. Lawrence, P. Liu, N. Watson, A.J. Sinskey, J.A. Stubbe, J. Bacteriol. (2005).
[69] WHO, Prevention and Control of Schistosomiasis and Soil-Transmitted Helminthiasis : Report of a WHO Expert Committee, 2002.
[70] H. Smith, M. Doenhoff, C. Aitken, W. Bailey, M. Ji, E. Dawson, H. Gilis, G. Spence, C. Alexander, T. van Gool, PLoS Negl. Trop. Dis. 6 (2012) e1815.
[71] D.G. Colley, S.K. Wikel, Exp. Parasitol. 35 (1974) 44–51.
[72] R.S. Curwen, P.D. Ashton, S. Sundaralingam, R.A. Wilson, Mol. Cell. Proteomics 5 (2006) 835–844.
[73] G.M. Knudsen, K.F. Medzihradszky, K.-C. Lim, E. Hansell, J.H. McKerrow, Mol. Cell. Proteomics 4 (2005) 1862–1875.
[74] J. Dvořák, P. Fajtová, L. Ulrychová, A. Leontovyč, L. Rojo-Arreola, B.M.

Suzuki, M. Horn, M. Mareš, C.S. Craik, C.R. Caffrey, A.J. O'Donoghue, Biochimie 122 (2016) 99–109.
[75] L. Hazell, L. Braun, M.R. Templeton, PLoS Negl. Trop. Dis. 13 (2019) e0007777.
[76] C.J. Shiff, S.K. Chandiwana, T. Graczyk, P. Chibatamoto, M. Bradley, J. Parasitol. 79 (1993) 149.
[77] A.A.M. Ahmed, A. Babiker, L.A. Eltash, C. Shiff, Acta Trop. 82 (2002) 363–368.
[78] S. Zaaijer, A. Gordon, D. Speyer, R. Piccone, S.C. Groen, Y. Erlich, Elife 6 (2017).
[79] B. Wolfenden, P. Boeing, Nat. Biotechnol. 34 (2016) 455–455.
[80] B. Berg, B. Cortazar, D. Tseng, H. Ozkan, S. Feng, Q. Wei, R.Y.-L. Chan, J. Burbano, Q. Farooqui, M. Lewinski, D. Di Carlo, O.B. Garner, A. Ozcan, ACS Nano 9 (2015) 7857–7866.
[81] K. Li, F.R. Tay, C.K.Y. Yiu, Pharmacol. Ther. 207 (2020) 107465.
[82] A. Remacle, J. Cell Sci. 116 (2003) 3905–3916.
[83] G.A. Conlon, G.I. Murray, J. Pathol. 247 (2019) 629–640.
[84] M.A. Cepeda, J.J.H. Pelling, C.L. Evered, K.C. Williams, Z. Freedman, I. Stan, J.A. Willson, H.S. Leong, S. Damjanovski, Mol. Cancer 15 (2016) 65.
[85] S. Kumar, B.I. Ratnikov, M.D. Kazanov, J.W. Smith, P. Cieplak, PLoS One 10 (2015) e0127877.
[86] P. Laudański, J. Swiatecka, L. Kozłowski, M. Leśniewska, M. Wojtukiewicz, S. Wołczyński, Folia Histochem. Cytobiol. 48 (2010).
[87] M. Shimoda, R. Khokha, Biochim. Biophys. Acta - Mol. Cell Res. 1864 (2017) 1989–2000.
[88] A. Das, V. Mohan, V.R. Krishnaswamy, I. Solomonov, I. Sagi, Cancer Metastasis Rev. 38 (2019) 455–468.
[89] G. Gonzalez-Avila, B. Sommer, D.A. Mendoza-Posada, C. Ramos, A.A. Garcia-Hernandez, R. Falfan-Valencia, Crit. Rev. Oncol. Hematol. 137 (2019) 57–83.
[90] D. Yang, Y. Liu, C. Bai, X. Wang, C.A. Powell, Cancer Lett. 468 (2020) 82–87.
[91] E. Groth, J. Pruessmeyer, A. Babendreyer, J. Schumacher, T. Pasqualon, D. Dreymueller, S. Higashiyama, I. Lorenzen, J. Grötzinger, D. Cataldo, A. Ludwig, Biochim. Biophys. Acta - Mol. Cell Res. 1863 (2016) 2795–2808.
[92] A. Dijkstra, D.S. Postma, J.A. Noordhoek, M.E. Lodewijk, H.F. Kauffman, N.H.T. ten Hacken, W. Timens, Virchows Arch. 454 (2009) 441–449.
[93] M.-E. Lalonde, Y. Durocher, J. Biotechnol. 251 (2017) 128–140.
[94] K.W. Yoo, N. Li, V. Makani, R.N. Singh, A. Atala, B. Lu, Tissue Eng. Part C Methods 24 (2018) 637–644.
[95] C.-H. Liu, P.-S. Wu, Biotechnol. Lett. 28 (2006) 1725–1730.
[96] J. Li, X. Chen, J. Yi, Y. Liu, D. Li, J. Wang, D. Hou, X. Jiang, J. Zhang, J. Wang, K. Zen, F. Yang, C.-Y. Zhang, Y. Zhang, PLoS One 11 (2016) e0163043.
[97] H. Li, E. Solomon, S. Duhachek Muggy, D. Sun, A. Zolkiewska, J. Biol. Chem. 286 (2011) 21500–21510.
[98] M. Uhlen, L. Fagerberg, B.M. Hallstrom, C. Lindskog, P. Oksvold, A. Mardinoglu, A. Sivertsson, C. Kampf, E. Sjostedt, A. Asplund, I. Olsson, K. Edlund, E. Lundberg, S. Navani, C.A.-K. Szigyarto, J. Odeberg, D. Djureinovic, J.O. Takanen, S. Hober, T. Alm, P.-H. Edqvist, H. Berling, H. Tegel, J. Mulder, J. Rockberg, P. Nilsson, J.M. Schwenk, M. Hamsten, K. von Feilitzen, M.

Forsberg, L. Persson, F. Johansson, M. Zwahlen, G. von Heijne, J. Nielsen, F. Ponten, Science (80-.). 347 (2015) 1260419–1260419.
[99] J.G. Pérez-Silva, Y. Español, G. Velasco, V. Quesada, Nucleic Acids Res. 44 (2016) D351–D355.
[100] A.A. Agbowuro, W.M. Huston, A.B. Gamble, J.D.A. Tyndall, Med. Res. Rev. 38 (2018) 1295–1331.
[101] N. Kurt Yilmaz, R. Swanstrom, C.A. Schiffer, Trends Microbiol. 24 (2016) 547–557.
[102] L. Zhang, D. Lin, X. Sun, U. Curth, C. Drosten, L. Sauerhering, S. Becker, K. Rox, R. Hilgenfeld, Science (80-.). (2020) eabb3405.
[103] V. Grum-Tokars, K. Ratia, A. Begaye, S.C. Baker, A.D. Mesecar, Virus Res. 133 (2008) 63–73.
[104] W. Rut, K. Groborz, L. Zhang, X. Sun, M. Zmudzinski, R. Hilgenfeld, M. Drag, BioRxiv (2020).
[105] J. Vandooren, G. Opdenakker, P.M. Loadman, D.R. Edwards, Adv. Drug Deliv. Rev. 97 (2016) 144–155.
[106] I.L.H. Ong, K.-L. Yang, Analyst 142 (2017) 1867–1881.
[107] G. Liu, J. Wang, D.S. Wunschel, Y. Lin, J. Am. Chem. Soc. 128 (2006) 12382–12383.
[108] P.A.M. Snoek-van Beurden, J.W. Von den Hoff, Biotechniques 38 (2005) 73–83.
[109] A.C. Mitchell, S.C. Alford, S.A. Hunter, D. Kannan, R.A. Parra Sperberg, C.H. Chang, J.R. Cochran, ACS Chem. Biol. 13 (2018) 66–72.
[110] T.G. Volova, S. V. Prudnikova, O.N. Vinogradova, D.A. Syrvacheva, E.I. Shishatskaya, Microb. Ecol. 73 (2017) 353–367.